INSTITUTE OF SCIENCES AND ENGINEERING

DEPARTMENT OF ELECTRICAL AND ELECTRONICS ENGINEERING

A SIMPLE LEAST SQUARES APPROACH FOR LOW SPEED PERFORMANCE ANALYSIS OF INDIRECT FOC INDUCTION MOTOR DRIVE USING LOW-RESOLUTION POSITION SENSOR

A Thesis

submitted by

SAEED UR REHMAN

in partial fulfillment of the requirements for the degree of

MASTER OF SCIENCE

April 2017

Program: Power Electronics and Clean Energy Systems

A SIMPLE LEAST SQUARES APPROACH FOR LOW SPEED PERFORMANCE ANALYSIS OF INDIRECT FOC INDUCTION MOTOR DRIVE USING LOW-RESOLUTION POSITION SENSOR

A Thesis

by

SAEED UR REHMAN

submitted to the Institute of Sciences and Engineering of

OKAN UNIVERSITY

in partial fulfillment of the requirements for the degree of

MASTER OF SCIENCE

Approved by:

Chair
Asst. Prof. Dr. S. Barış ÖZTÜRK
Supervisor

Prof. Dr. R. Nejat TUNCAY
Member

Assoc. Prof. Dr. Özgür ÜSTÜN
Member

April 2017

Program: Power Electronics and Clean Energy Systems

ABSTRACT

A SIMPLE LEAST SQUARES APPROACH FOR LOW SPEED PERFORMANCE ANALYSIS OF INDIRECT FOC INDUCTION MOTOR DRIVE USING LOW-RESOLUTION POSITION SENSOR

The main objective of this project is to achieve very low speed three phase ac motor field oriented control using least mean square approach with low resolution encoder under full load condition. The common usage and demand of electric machines brings the need of position sensors. Although position sensorless algorithms have been developed and used recently, but safe and sensitive operation of electric machines require position sensors. In the market, there are encoders with various price ranges. These prices vary depending on brand, model and resolution of the encoder. High resolution encoders (256–2048 ppr) have high prices which ranges between 100 TL and 1000 TL and they provide good low speed performance. However, although low count encoders have low price between 20 TL and 100 TL, but do not perform low speed operation very well. The aim of proposed project is to obtain a motor control system with low-price, low-count incremental encoder at very low speed replacing high-price, high-resolution encoders saving money for the companies.

The novelty of this project is to use a linear least square algorithm for IFOC of AC motors (PMSM & IM) in processing of low count encoder signals at low speeds under full load conditions.

Keywords: LLS, Indirect Field Oriented Control, Permanent magnet synchronous motor, Induction motor, Incremental encoders,

KISA ÖZET

ASENKRON MOTORUN DOĞRUDAN OLMAYAN ALAN ETKİLİ VEKTÖR KONTROLÜ İLE DÜŞÜK ÇÖZÜNÜRLÜKLÜ ENKODER KULLANILARAK DOĞRUSAL EN KÜÇÜK KARESEL YAKLAŞIM YÖNTEMİYLE DÜŞÜK HIZLARDAKİ PERFORMANS ANALİZİ

Bu projenin temel amacı, 3 fazlı alternatif akım motorunun maksimum yük koşulu altında ve düşük çözünürlüklü enkoder ile çok düşük hızlarda, küçük kareler yaklaşım metodunu kullanarak alan yönlendirmeli vektör kontrolünü yapabilmektir. Elektrikli makinelerin yaygın kullanımı ve talebi, pozisyon sensörlerinin ihtiyacını beraberinde getirmiştir. Son zamanlarda pozisyon sensörsüz algoritmaların geliştirilip kullanılmasına rağmen, elektrikli makinelerin güvenli ve hassas çalışabilmesi için pozisyon sensörlerinin kullanımı gereklidir. Piyasada çeşitli fiyat aralıklarında enkoderler vardır. Bu fiyatlar enkoderlerin marka, model ve çözünürlüğüne bağlı olarak değişir. Yüksek çözünürlüklü enkoderler (256–2048 darbe sayısı), 100 TL ile 1000 TL arasında değişen yüksek fiyatlara sahiptir ve düşük hızlarda iyi performans gösterirler. Bununla beraber, düşük darbe sayılı enkoderlerin fiyatı 20 TL ila 100 TL arasında olmasına rağmen, düşük hızlarda iyi performans gösterememektedir. Önerilen projenin amacı, düşük fiyatlı, düşük darbe sayılı, artımsal enkoderli, çok yüksek hızlarda, yüksek çözünürlüklü enkoderler yerine şirketlere para kazandıran bir motor kontrol sistemi elde etmektir.

Bu projenin yeniliği, maksimum yük koşullarında, düşük hızlarda, düşük darbe sayılı enkoder sinyallerinin işlenmesinde alternatif akım motorlarının doğrudan

olmayan alan etkili vektör kontrölü için doğrusal en küçük kareler algoritmasını kullanmaktır.

Anahtar Kelimeler: Doğrusal En Küçük Karesel, Doğrudan Olmayan Alan Etkili Vektör Kontrolü, Kalıcı Mıknatıslı Senkron Motor, Asenkron Motor, Artımsal Enkoder

To my parents, brothers, wife and my son.

ACKNOWLEDGMENT

There is a numerous amount of people I need to thank for their advice, help, assistance and encouragement throughout the completion of this thesis.

First of all, I would like to thank my advisor, Asst. Prof. Dr. Salih Barış Öztürk, for his support, continuous help, patience, understanding and willingness throughout the period of the research to which this thesis relates. Moreover, spending his precious time with me is appreciated far more than I have words to express. I am very grateful to work with such a knowledgeable and insightful professor. To me he is more than a professor; he is like an elder caring for his students during their education. Before pursuing graduate education in the Turkey I spent a great amount of time finding a good and quality professor to work with. Even before working with Prof. Barış I realized that the person who you work with is more important than the prestige at the university in which you attend.

I would like to extend my gratitude to my fellow colleagues in the Power Electronics and Energy Conversion (PEEC) Laboratory: Asst. Prof. Dr. Ömer Cihan Kıvanç, Ibrahim, Berkin Atila, Muhammad Ameen Majeed and Saim Mukhtar Hussain. I cherish their friendship and the good memories I have had with them since my arrival at Okan University.

Also, I would like to thank to the people who are not participants of our lab but who are my close friends and mentors who helped, guided, assisted and advised me during the completion of this thesis: Dr. Khawar Nadeem, Zia Ur Rahman, Shams Ur Rahman, Shah Khalid, Ihsan Ullah, Aamir Samim Arabzai, Usama Bashir Randhawa,

Ghouse Ali, Abdur Rahman Niazi, Ilyas Kaka Khel, Farhan Danish, Khurram Sajjad and many others whom I could not mention here.

I would also like to acknowledge the Electrical Engineering department staff at Okan University: Prof. Ramazan Nejat Tuncay, Assoc. Prof. Dr. Burak Kelleci, Asst. Prof. Dr. Didem Kıvanç Türeli, and many others for providing an enjoyable and educational atmosphere.

Last but not least, I would like to thank my parents and my wife for their patience, and more importantly, moral support throughout my life. First, I am very grateful to my dad for giving me the idea, opportunity and financial support to study abroad to earn a good education. Secondly, I am very grateful to my mother for her patience which gave me a glimpse of how strong she is. Even though they do not show their emotion when I talk to them, I can sense how much they miss me when I am away from them. No matter how far away from home I am, they are always there to support and assist me. Finally, to my parents, no words can express my gratitude for you and all the things you sacrifice for me.

TABLE OF CONTENTS

LIST OF TABLES

LIST OF FIGURES

SYMBOLS

α	Alpha
β	Beta
ϕ	Phase Angle
θ	Electrical Angle
ω	Speed
φ	Air gap Flux
λ	Flux Linkage
$\sum$	Summation
Δ	Delta
μ	Micro

ABBREVIATIONS

ACI Alternating Current Induction Motor

PMSM Permanent Magnet Synchronous Motor

FOC Field Oriented Control

IFOC Indirect Field Oriented Control

DSP Digital Signal Processor

LSM Least Square Method

OLS Ordinary Least Square

WLS Weighted Least Square

PLS Partial Least Square

ALS Alternating Least Square

LLS Linear Least Square

EMI Electro-Magnetic Induction

QEP Quadrature Encoder Pulse

CAP Capture Unit

SVPWM Space Vector Pulse Width Modulation

I. INTRODUCTION

1.1. Principles of AC Machines

AC machines operate on a basic principle i.e. the generation of a rotating magnetic field which tends to rotate the rotor part of the motor and turn at a speed relative to the speed of rotation of stator magnetic field. AC currents are the main source of generation of rotating magnetic field in the stator and air gap of the motor.

In Figure I.1, stator coils are geometrically placed at an angle of 120° with a three-phase input supply voltage and with windings configuration *a–a'*, *b–b'* and *c–c'*. Likewise, the currents generated by the 3–ϕ supply voltage source are also spaced by 120° phase shift.

The following equations symbolizes the neutral terminal with a referenced phase voltages [1]:

$$v_a = A\ \cos\ (\omega_e t) \tag{I.1}$$

$$v_b = A\,cos\ \ (\omega_e t - \frac{2\pi}{3}) \tag{I.2}$$

$$v_c\ = A\,cos\ \ (\omega_e t + \frac{2\pi}{3}) \tag{I.3}$$

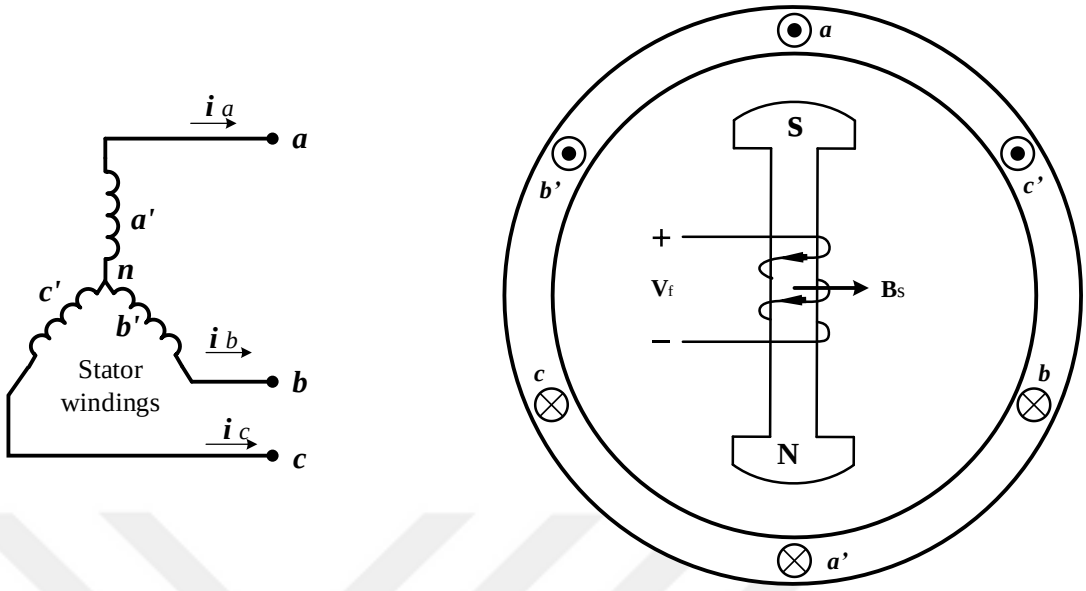

Figure I.1. Two-pole 3–ϕ stator with its windings.

where ω_e is the frequency of the input AC supply. The approximate sinusoidal varying flux distribution is generated by an appropriate and elegantly arranged coils in each winding over the stator surface. So, the sum of the fluxes in each separate winding with coils spaced by an angle of 120° as well as a sinusoidally varying flux distribution. Thus, the flux in a 3–ϕ motor will revolve in space according to its vector diagram.

The frequency of the sinusoidal phase currents must be related to the speed of the resultant flux rotation. Similarly, in Figure I.1, the stator has two magnetic pole following its winding configuration and other machines can be configured to have more than two poles.

The equation below shows the frequency of the excitation current and the number of poles present in the stator, expressing the speed of the rotating magnetic field in general [2].

$$n_s = \frac{120\ f}{p}\ \ rpm \tag{I.4}$$

$$\omega_s = \frac{2\pi n_s}{60} = \frac{2\pi \times 2f}{p} \tag{I.5}$$

where n_s is generally termed as the synchronous speed.

It is noteworthy that the major difference between AC machines that whether it is a generator or a motor depends on the direction of the power flow. The electromagnetic torque in a generator is a reaction torque that opposes the machine rotation and the prime mover works against this torque. And the rotational voltage (also called the back emf) generated in the armature coils of the motor opposes the voltage applied.

As we know that in ACI motor the magnetic field generated in the rotor cannot catch up the magnetic field in the stator due the slip of the motor. The number of magnetic poles in the stator and rotor depends on the speed of rotor rotation. Furthermore, the angle θ between the rotor and stator magnetic fields represents the magnitude of the torque produced (which is determined precisely by the generation of magnetic fields) in both the synchronous and induction machines. For a constant electromagnetic torque to be generated, it is necessary in all rotating machines that the number of poles in stator and rotor must be identical and even. On the contrary, these constant-torque machine give rise to torque pulsation which in turn results mechanical vibration in the machine and its other attached mechanical components like belts, load etc. Nevertheless, these vibrations must be ignored which is quiet a hard task. This can be done by accomplishing multiphase excitation currents which gives rise to a constant and uniform torque and produce a constant flux per pole.

1.2. AC Motors and Their Trends

AC motors are known to be the suitable machines for most of the customers in the market with light weight and inertia means rugged like permanent magnet synchronous motors (PMSM) and induction motors (IM). The salient features of these AC motors over DC motors are [3]:

- They are autonomous in terms of an electrical connection between motor parts.
- Without any mechanical commutator and brushes.
- Extremely effective, inexpensive, mechanically convenient and have capability of high overload.
- Employ a simple and proficient electromechanical energy conversion.
- Operates at variable speeds with a variable amplitude and frequency of three phase source.

The speed of the rotor totally based on the stator magnetic field speed which rotates at the frequency of the voltage applied. While variable speed is inversely proportional to the coupled torque and flux. In the same manner, a variable voltage at low frequencies is of prime importance [4]. In early ages, in spite of using direct torque and vector control schemes of AC machines, traditional methods were not suitable for variable speed applications just because of the coupled flux and torque within the motor means varying one will affect the other.

Another control method of induction motors was also achieved earlier at very limited speed by switching from $3-\phi$ delta to star connection which makes the voltage decreased in the motor windings. Poles of the motor can be changed by if the motor has

more then 3-phases, but these are capable for discrete speeds. Therefore this speed control method is more costly and inefficient if a motor has several stator windings [1].

So, in order to achieve speed control an alternative method is adopted by utilizing wound rotor induction motor in which the windings of the rotor are attached to slip rings. Though, it resulted in the reduced and poor performance [5].

The aforementioned methods were being utilized in previous decades for speed control of induction motors which was not better than DC motors in terms of torque performance and high speed high speeds [1].

With the emergence and development of fast and cost-effective microprocessor (based on advanced control algorithms rather than complicated hardware control) and DSPs, the adjustable speed drives can be provided easily and it also allows independent control of flux and torque in ACI motors achieving good characteristics of linear torque as compared to DC motors.

1.3. Induction Motors

Three-phase induction motors are most widely used in the industries, offices and homes etc. just because of the genius Nikola Tesla who invented this novelty, the Induction Motor also called the asynchronous motor in 1983. The two main types are wound and squirrel-cage induction motors. But squirrel cage IM is mainly used as it has a high demand as compared to wound type IM in certain features such as ruggedness, remoteness of the rotor, zero resistance, reliability, lack of wiring and expediency in usage. Mostly induction motors are independent in terms of speed in relation to torque. As there are no moving contacts like brushes and commutators in squirrel cage IM, it greatly affects the reliability and performance of IM and getting rid of the sparking issue, means reliable to use it in the harsh environments. Looking at the

rugged construction of the rotor squirrel cage IM is capable of taking heavy loads as shown in Figure I.2 below.

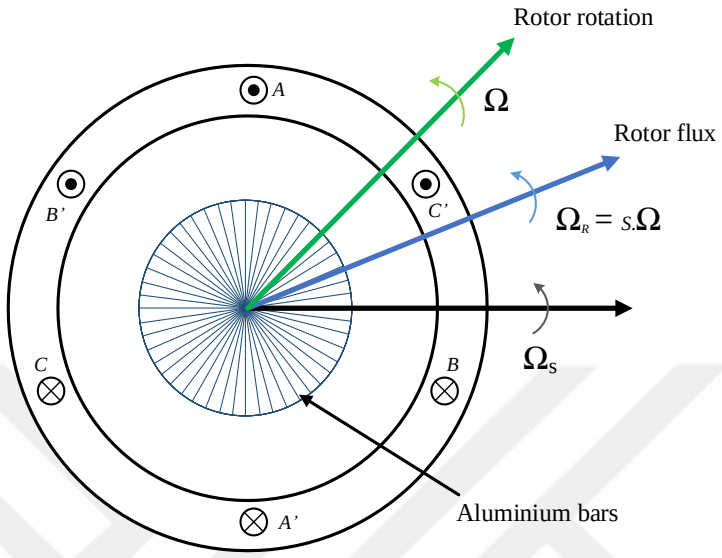

Figure I.2. Cutaway view of squirrel cage ACI motor.

However, the rarely used wound-rotor induction motors which is almost phased out from the industries have certain characters such as costly and less reliable. In wound IM, the winding of rotor is attached with the brushes and slip rings over the stator. Generally, the motor current is reduced via adjustable resistors (rheostats). On the other hand, adjustable speed control is accessed in the so-called cascade systems, based on the reduction of extra power supply and its return to the supply line. Today's high-efficiency motors such as those used for machine tools or elevators are smaller and reliable in terms of energy consumption beside their luxuriousness and assuming average life span of IM of twelve years with proper maintenance which is much higher than other applications with less life span [5].

1.4. Induction Motor Drive Systems and Its Applications

Electric drive system consists of an electric motor which drives a mechanical load connected in line to its shaft directly or through a gearbox (or v-belt) transmission along with its corresponding control equipment i.e. switches, sensors, microprocessors, power converters, and relays. These equipment's combined together constitute an electric drive system. Even nowadays some of the induction motors are functionally uncontrolled (only limited to on and off switching) without a drive system means no control resulting very low efficiency. However, ASDs with induction motors are mostly common in industries due to a high torque and inertia and compete with the DC drives.

Some of the most common examples of induction motors are blowers, compressors, fans, grinders and pumps. However, all of these have a certain limited speed control despite of using high dynamic performance drives. Let say a blower with a constant speed would reduce its speed and torque if the air outlet is choked during an uncontrolled condition. High-performance induction motors with adjustable speed drives are used in terms of improved performances, like in elevators which require torque and position control precisely, and also these are utilized in electric vehicles and electrical tractions etc. An induction motor ASD must include an inverter (which is a variable-frequency source). It is also called DC to ac converters, in which AC from power line is supplied to a rectifier which give DC power. It also consists of a capacitor or reactor between rectifier and inverter and known as DC link.

Rectifiers perform a role in drawing distorted, non-sinusoidal currents from the input power system in association with active or passive filters to decrease the supply current low frequency harmonic part. While inverters produce high frequency current noise, and the system should be protected from these noises. If it's not blocked then the

overall electromagnetic interference (EMI) might disturb the sensitive communication and control equipment operations. Thus, for this purpose efficient EMI filters are desired as well. Microcontrollers, digital signal processors (DSPs), and microcomputers are most commonly utilized in controlling of adjustable speed drives (ASDs). On the contrarily, an ASD became much more multifaceted and costly than uncontrolled motors when installed with associated current, voltage, speed, or position sensors. On the other hand, certain competent, consistent, and user-friendly systems in the motion-control industry would compete with the present ASDs with induction motors in terms of various industrial applications.

1.5. Outline of the Thesis

Induction motors have been the first choice for a wide variety of industrial applications for many years due to their robust and rugged structures. Previously, induction motors were driven either directly from the grid or by volts/hertz (scalar) control. They have the advantage that little information about the motor is needed to make them operate properly. On the other hand, these methods have some drawbacks such as the speed control provided by these methods supporting a wide range of applications does not cover some high-end applications that require a torque source.

The preference of using induction motors is very much improved with the advent of field oriented control schemes in which control of induction motor can mimic separately excited DC motors. This allows the induction motor’s stator current to be separated into a flux-producing component, analogous to a DC machine field current and armature current. The indirect field oriented control (vector control) for speed and torque controlled ac drives are becoming the industry standards to obtain high dynamic performance.

Recently, many research groups have investigated the possibility of rotor position sensorless control of induction motor [6], [7] and [8]. Although these algorithms provide satisfactory speed estimation at high speed range, sluggish performance is observed at low speed due to various problems such as measurement offsets, voltage drops on the switches, parameter deviations, etc. Thus, to enhance the reliability of overall system in drive technology, companies prefer position sensor-based control techniques [9], [10]. Since the high resolution encoders are quite expensive, companies tend to employ low-cost, low-resolution encoders for field-orient control (FOC) of AC drives [9]. In this thesis, a further progress is achieved and is experimentally proved that the bulky and expensive medium and high resolution incremental position encoders ($100 to $300) can be replaced by cheap low-count (low- resolution) incremental encoders (<$10) and permanent magnet integrated hall-effect sensors (<$2) safely even at very low speed.

First of all, a low-count encoder implementation algorithm is developed to test the lowest possible pulse encoder that pro-vides both precise speed information and satisfactory performance for IFOC of IM drive. Using this algorithm, different numbers of pulse encoders are tested and the lowest possible pulse encoder is selected for IFOC implementation due to the cost limitation. Furthermore, solutions to computational problems of the micro-processing unit associated with the low speed measurement techniques are given. It is well known that low-count encoders provide satisfactory results at high speed range. However, at low speeds (depending on the number of encoder pulses) significant errors are observed. One reason of this failure is because of keeping the previous speed sample until the next position update [9]–[11]. Therefore, an erroneous peed is fed back to the overall control system and generally oscillatory or

even uncontrollable speed result is obtained especially at low speed conditions (1–5 rpm) [9].

In Chapter V, an ordinary least squares (OLS) speed estimation algorithm (linear and quadratic) is suggested to achieve better speed performance at very low speed by using low-count encoders. In the proposed method, predetermined numbers of speed data sets are best fit by both linear and quadratic least squares algorithms such that more realistic speed results can be achieved. Experimental tests and results in Chapter VI, show that when OLS speed estimation is used quite satisfactory speed responds are observed. Those results demonstrate the superiority of the OLS speed estimation on low speed performance for IFOC of IM drive by using the low-count encoders compared to the common techniques.

II. ENCODERS & SENSORS

A sensor is device which has the ability of quantitatively measuring a certain physical quantity. In applications of motor controls, the primary sensors which are used in electric drives consists of speed/velocity, torque, acceleration and position sensors. The sensors are mainly divided into two categories, Optical and Non-Optical sensors [12]. Optical sensors include autocollimators, optical encoders, fiber optic sensors, interferometric sensors, laser triangulation sensors. Non-optical sensors include Hall-effect sensors, inductive digital on/off proximity sensors, inductive distance measuring sensors, Magnetic scales, magnetostrictive sensors, potentiometers, LVD (linear variable differential) and velocity sensors.

For measuring position, the sensor can either be an absolute sensor or the displacement sensor. These sensors may be linear, angular or multi-axis. Common types of position sensors includes the potentiometer, LVDT, encoder, Hall-effect sensors [13] etc. we will discuss the one we are using in this project and some of them as well briefly here.

2.1. Encoders

Encoder is a sensor of mechanical motion which generates digital signals as a result of a displacement. It’s an electro-mechanical device as shown in Figure II.1, which is able to provide the motion control system users with information like position, velocity/speed, and direction. There are two basic types of encoders: Linear and Rotary encoders.

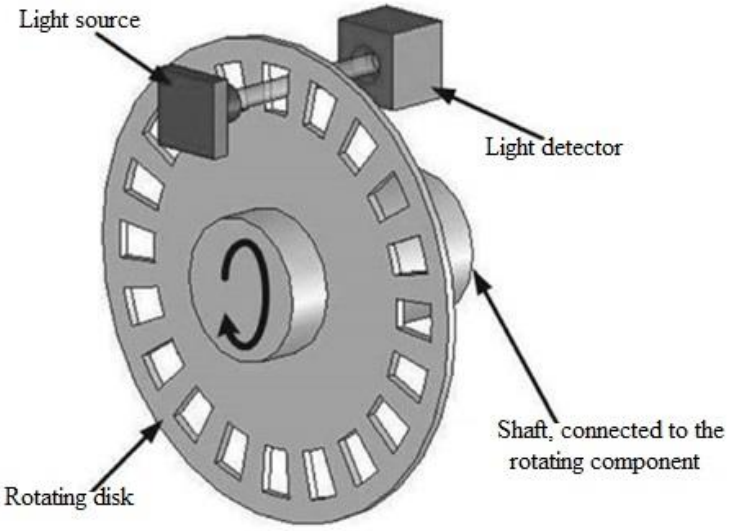

Figure II.1. Inside of an optical encoder.

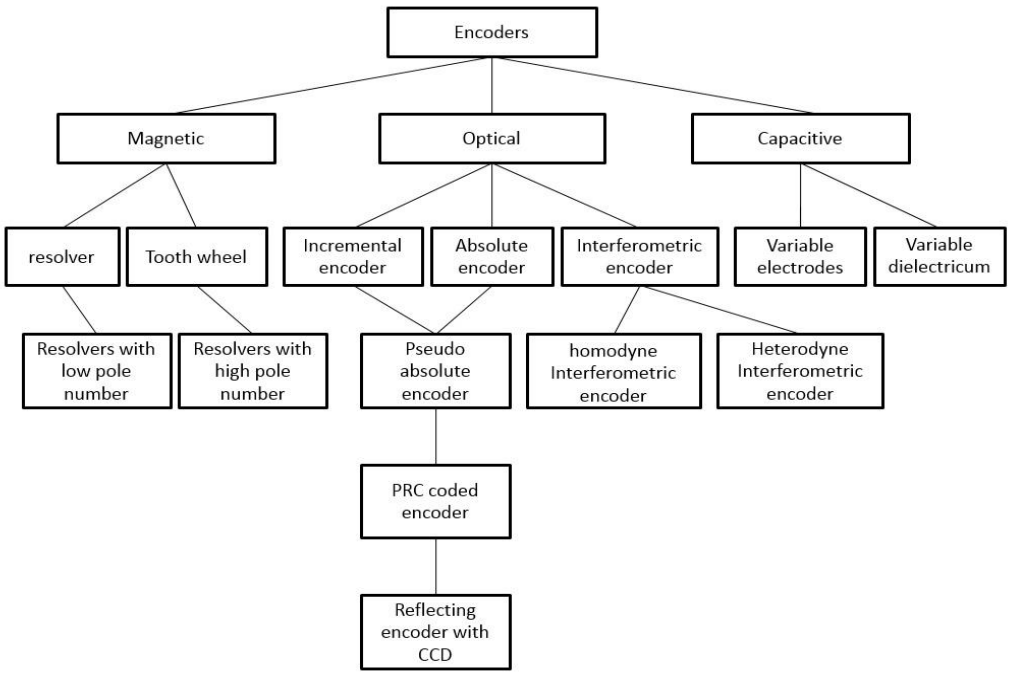

Figure II.2. Position encoders in servo drives [14].

2.1.1. Linear Encoders

Linear displacement can be measured and evaluated by a device called encoder whose basic output signals are in digital format, so there is no need of conversion from analog-to digital. Linear encoders can be incremental or absolute, and uses some detection techniques, which includes capacitive, brush, magnetic and optical types [15].

2.1.1.1. Advantages of Linear Encoders

Linear encoders such as incremental transducers and magnetic linear encoders are often considered as an ideal candidate for precision (with a resolution as fine as 0.01 mm) and long range (up to 40 m) and non-contact measurement of the position sensing method. On the contrary, incremental mode has certain limitation like electromagnetic noise or power fluctuation can cause data corruption. Magnetic linear encoders have reliability and long lifespan. Shorter linear encoders can be magnetically or optically coupled and are self-contained with the magnetic tape or optical scale enclosed within a housing. Typical linear encoder used in the industries has a resolution of more than 0.1 mm. The bushings and wipers, utilized in models having an actuator rod with a finite lifetime and can cause audible noises with the passage of time, rather than affecting measurement accuracy.

The position information of an encoder is further categorized as [15]:

1. Incremental encoder, which detects motion (displacement) from some point.
2. Absolute encoder, which detects the actual position of the encoder.

2.1.2. Absolute vs Incremental Encoders

An absolute encoder generally encodes sufficient information from many number (requiring more bits) totally present at the same position. On the other hand, in

incremental encoders only one or two bits of information are located at each point with alternative position. Furthermore, an incremental encoder may also have an index track with a marked starting point (where the count can be reset automatically after each interval). Therefore, incremental encoder may have more advantage over absolute one as they are used as higher resolution for a given spacing of the detected feature. In general, number of bits are inversely proportional to the resolution. On the contrary, an absolute encoder without reset to zero count has the advantage of instant startup after a corruption of power or data [15].

2.1.3. Optical Encoders

An optical encoder comprised of a transmitted part (light source usually a light-emitting diode) that includes a focusing lens, collimator, and a slit or pinhole, a receiver part (usually a phototransistor) and a strip having opaque (dark area) and transparent (light area) sections arranged in a row as shown in Figure II.3. The light source focus light on detector for detection (through counting) of the present position. A closer spacing between adjacent dark or light areas will yield a higher resolution. The optical encoder can be incremental or absolute.

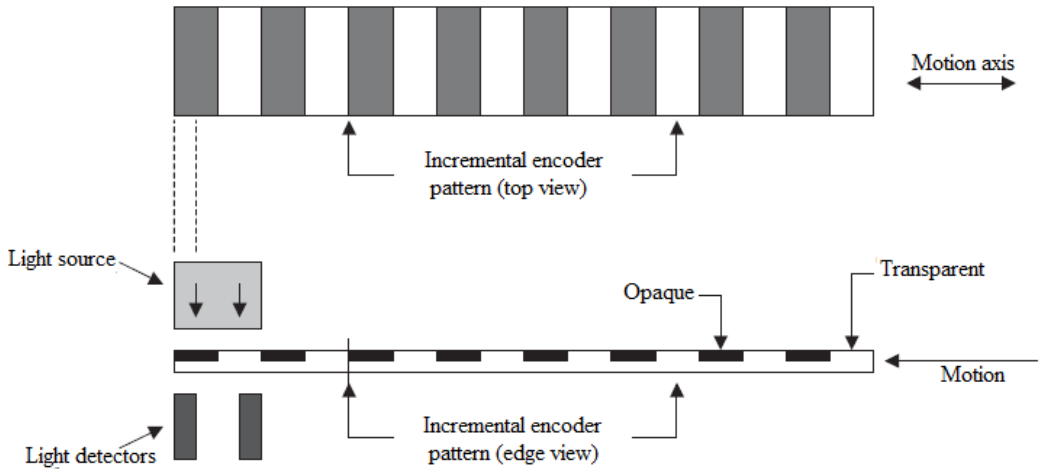

Figure II.3. Incremental optical encoder with LED and phototransistor.

2.1.4. Magnetic Encoders

A magnetic encoder mainly consists of a magnetic tape (for position information) and one or more magnetic sensor (for data reading) which are of Hall Effect or magneto resistive type. The magnetic encoder can be incremental or absolute. An incremental magnetic encoder in Figure II.4, consist of a magnetic tape having reversals of polarization along its length and the magneto resistive pickups (only two) for the detection of magnetic field variations. In addition, the second pickup pair resulting in a quadrature output count pulses from the present position. The absolute magnetic encoder is presented in Figure II.5, following the same concept as represented for the optical type.

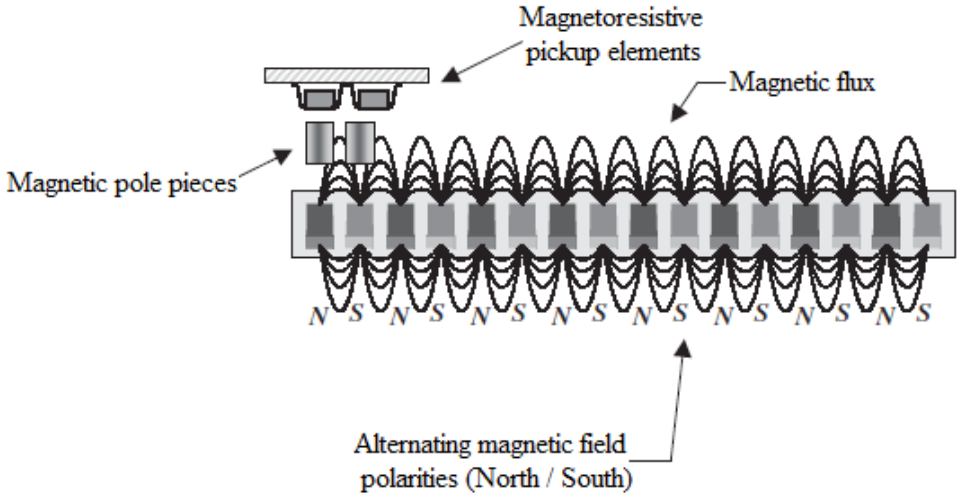

Figure II.4. Incremental magnetic encoder with magneto resistive pickup.

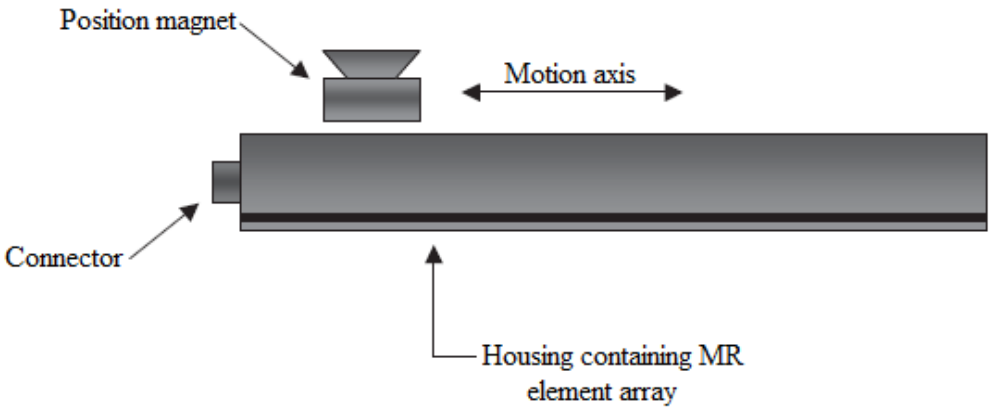

Figure II.5. Absolute magnetic encoder.

2.1.5. Quadrature

Incremental encoders consist of two outputs, called A and B, which are arranged in quadrature (means they are separated in phase by 90°) and it also known as A quad B. It is called quadrature because it occurs with four transition per count cycle (comprise of 360°, which is a count cycle rather than the angle of rotation of a rotary sensor) and four possible states such as (1) A high, B low; (2) A high, B high; (3) A low, B high; and (4) A low, B low [9]. The change in position can be determined from the following equation:

The change in position= the number of counts × the distance per count.

The second output (B or A) represents the direction of motion, either incrementing (A goes from low to high while B remains low) or decrementing (A goes from low to high and B is also high at that time) the count as shown in Figure II.6. Modern circuits in which that read the A quad B signals actually monitor state from a position transducer, rather than transition for smoother operation with minimal error [15].

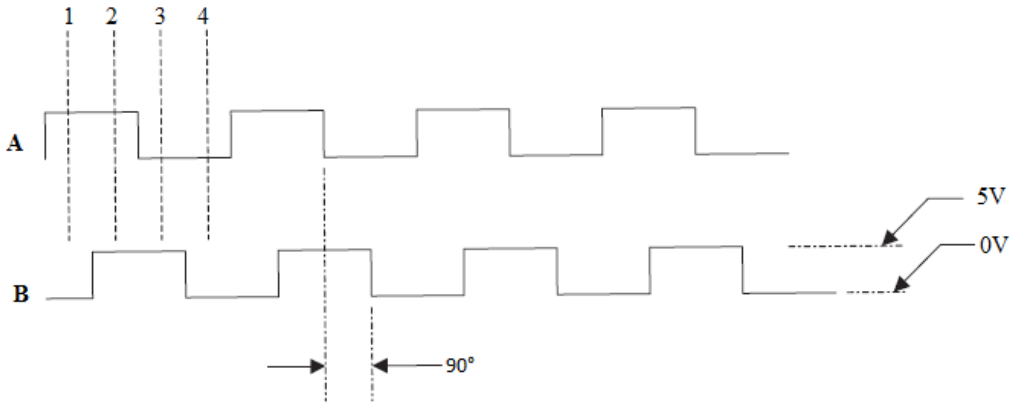

Figure II.6. A quad B outputs are separated by 90°. States 1 through 4 occur during each count cycle.

2.1.6. The Resolver Sensor

The resolver is a rotary position sensor which has benefited the industry for more than five decades. Basically, it was developed for military purpose applications. They are particularly employed in product packaging plants, stamping press lines and military applications. In some applications, the resolver fetches position data and feeds it to a decoder in programmable logic controller (PLC), which interprets the information and executing commands based on machines position.

Figure II.7 represents the basic operation of a resolver. In this figure, the resolver (a transmitter unit), consist of three different coil windings: the reference, the sine (SIN), and the cosine (COS). The reference winding is the primary winding which is energized on its primary side by an AC voltage through a transformer (also known as rotary transformer). This voltage is then passed from the primary to the secondary side of the transformer with no need of brushes and rings, which in turn increases the overall robustness and strength of the resolver. As the motor or reference winding mounted on the shaft spins, the voltage output from the SIN and COS windings as well as its angle (the theta rotation angle or θ) of difference change according to the shaft position. The induced voltages in SIN and COS windings is approximately equal to the reference voltage multiplied by the angle of SIN and COS windings [16].

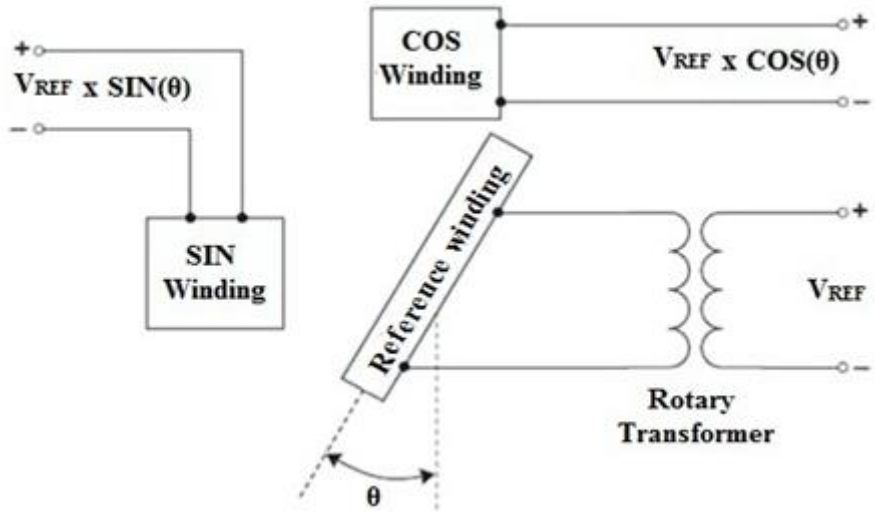

Figure II.7. Simplified mechanical schematic of a resolver transmitter unit.

2.1.7. Hall-Effect Sensors

First practical application was done as a microwave power sensor in 1950's. With increasing production of semiconductors, it is now very familiar to use Hall Effect in high volume products. Nowadays, Hall Effect sensors are mainly used in automotive and industrial products due to its long-life capability as well as its cost effectiveness, and included in many products like from automobiles to aircraft, machine tools to medical equipment, and computers to sewing machines, and motion control systems.

It's like an ideal sensing technology. It's a magnetic field sensor and it is used in many types of sensing devices like temperature, position, current, and pressure as a principle component.

It is constructed from thin sheet of conductive material having output connections which are perpendicular to the direction of current flow. When the current carrying conductor is subjected to the magnetic field, it experiences an output voltage which is proportional to the magnetic field strength. This output voltage is very small (in μV)

and it requires some additional electronics to achieve useful voltage levels. So it means when the Hall element is combined with the associated electronics, it makes a Hall Effect sensor [17].

Hall effect based sensing devices have some general features [17]:

- True solid state
- Operates with stationary input (zero speed)
- No moving parts
- Logic compatible input and output
- Temperature range (-40 to +150ºC)
- Repeatable operations
- Long life (30 billion operations keyboard module test program)
- High speed operations (over 100 kHz)

2.1.7.1. Hall Effect

Hall-effect was discovered by Dr. Edwin Hall in 1879. He discovered that, when a conductor carrying current is placed in a magnetic field. The result is voltage production which is perpendicular to the current and magnetic field as well as shown in Figure II.8 shown below. This principle is called Hall Effect [12].

The Figure II.8, illustrates the basic principle of Hall Effect. A thin sheet of semiconductor material (also called the Hall element) through which the current is passed. Output connections are perpendicular to the direction of current. When there is no magnetic field, the current distribution is uniform and no potential difference is produced at the output as shown in the figure below. Now if the current carrying conductor is placed near magnetic field, then there will be a force exerted on the current called Lorentz force [17]. This force will disturb the current distribution which results

in a potential (voltage) difference at the output. This voltage is called the Hall voltage (VH). The current and magnetic field interaction is shown in equation below:

$$VH \propto I \times B$$

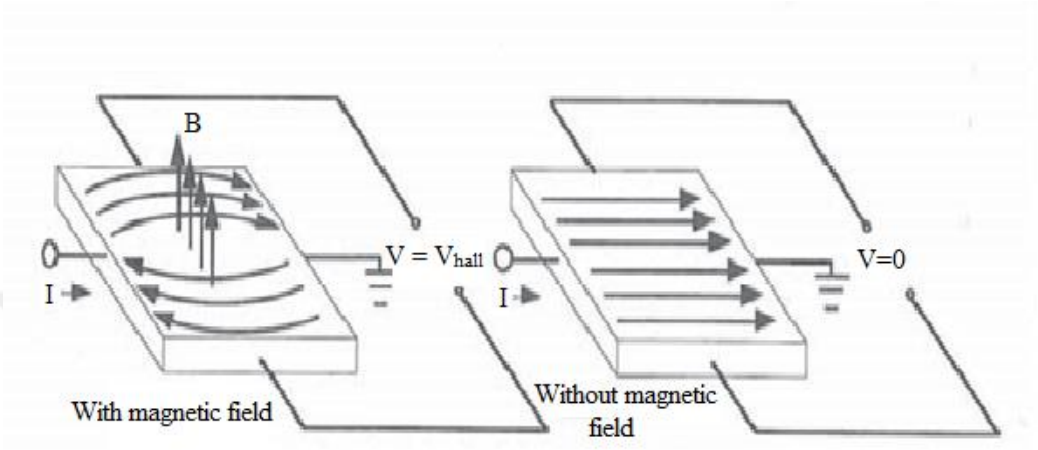

Figure II.8. Operating principle of a Hall Effect sensor [12].

III. SENSORED INDIRECT FIELD ORIENTED CONTROL OF 3-PHASE INDUCTION MOTORS

A cost-effective, compact and efficient solution has been devised in order to integrate a 3 phased AC induction motor using the TMS320F2803x devices that belongs to the family of C2000 microcontrollers [18]. These microcontrollers were implemented for the encouragement of precise digital vector control algorithms like the Field Orientated Control (FOC) which is discussed below. The FOC algorithm works on a certain principal i.e. in a dynamic model of the motor efficiency became directly proportional to a controlled speed and in the same manner torque alteration occur with transient phases. A brief background on field oriented motor control principle are discussed below.

The motor control industry is considered to be a dynamic industry where advanced control algorithms (through embedded control technology) play an important role in terms of high efficacy and minimizing the cost, work force, power consumption, EMI radiation and especially compete with its contemporary industries. It is notable that most of the industries use AC induction motor due to its high performance and dependability. Beside all these importance and robustness, AC motors have several constraints like having complex mathematical models, non-linear behavior, unable to control and temperature-dependent electrical parameter oscillation. So, in order to overcome all these limitations, it is necessary to use a certain control algorithm like vector control along with a highly efficient microcontroller for algorithm execution. With the advent of microcontrollers, the development of electronic industries with

controlled electric drives started increasing. Furthermore, these technological improvements in turns produced more accurate and highly efficient AC drive control. One of the vector control scheme termed as the Field Orientated Control method is discussed here. This scheme is totally dependent on three main points which are as under:

- The machine current and voltage space vectors
- Three phase speed is transformed, and
- Transformation of time dependent system into a two coordinate time invariant system and effective SVPWM pattern generation.

3.1. Field Oriented Control (FOC)

Due to the microcontrollers innovation in the AC induction motors, field oriented control is considered to be the most advanced and dynamic control system in term of efficiency and performance. These microcontroller uses mathematical transformations to decouple the generation of torque and the magnetic field functions in an AC induction motor [19], which is also called rotor flux oriented control, or simply Field Oriented Control (FOC).

The main philosophy behind the FOC role in AC induction motors is based on a principle in which the flux and torque are independently controlled and the current through the rotor windings regulates torque production.

It is important to note that the control of AC induction motors is totally different from that of the DC motor in terms of stator currents. In the synchronous motors, the rotor is excited by the mounted permanent magnets onto the shaft and the source of power and magnetic field is the stator voltage. The key function of FOC (also termed

as vector control) in both type of synchronous and asynchronous motors is to independently control the torque production and magnetizing flux.

3.1.1. Why Field Oriented Control?

Field oriented control technique may be adopted due to the following:

- FOC decouple the torque and magnetizing flux effect.
- They are thought to control torque independently to maintain the speed.
- They have efficient processing capability that enables these mathematical transformations quickly.
- They encourage and enable higher performance by executing the entire algorithm controlling the motor.
- They have better overall control credibility.

3.1.2. Technical Background

The Field Orientated Control works on a principle in order to control the stator currents which is represented by a vector. This control consists of projections and subsequently transformation of a 3−ϕ time and speed dependent system into a two coordinate (d and q) time invariant system. These projections imitate DC machine control structure.

Field orientated controlled motors consists of two input reference constants i.e.

a. The torque component (aligned with the q−coordinate).

b. The flux component (aligned with d−coordinate).

Field Orientated Control works independently and accurately in steady and transient state and thus explains the classic scheme complications, in the following ways:

• The easiness of approaching to constant torque and flux component references of the stator current.

• The direct torque control can be easily applied because the expression of the torque in (d, q) reference frame is:

$$m \propto \psi_R \, i_{sq} \tag{III.1}$$

As it is obvious from the equation that if the rotor flux (ψ_R) amplitude at a fixed value is maintained, the linear relationship between torque and torque component (i_{sq}) will occur. Then we can manage to control the torque by controlling the torque component of current stator vector.

3.2. Space Vector Definitions and Its Projection

Complex space vector denotes the analyzed three-phase voltages, currents and fluxes of AC-motors. In terms of currents, the space vector can be well-defined as under:

$$\overline{i_s} = i_a + \alpha i_b + \ a^2 i_c \tag{III.2}$$

Assume that i_a , i_b and i_c are the instantaneous currents in the stator phases, then the complex stator current vector is represented in Figure III.1:

Whereas, $\alpha = e^{j\frac{2}{3}\pi}$ & $\alpha^2 = e^{j\frac{4}{3}\pi}$ represents spatial operators. Figure underneath shows the stator current space vectors:

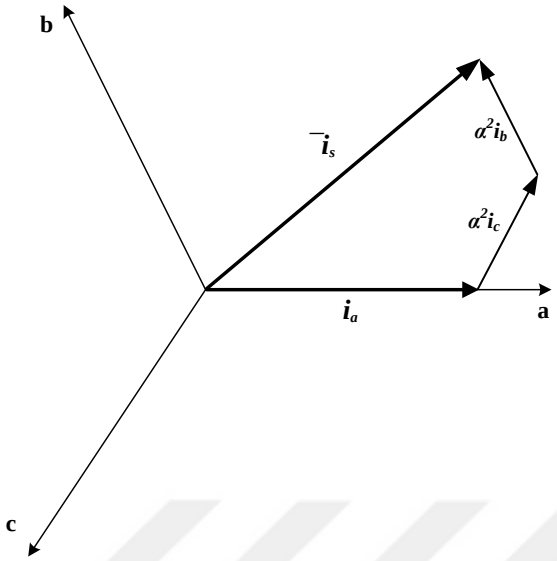

Figure III.1. Stator current space vectors and its components in (a, b, c).

where (a, b, c) are the 3–ϕ system axes. This current space vector denotes the 3–ϕ sinusoidal system which needs transformation into a two time independent coordinate system. This transformation can be divided into two stages [19]:

- $a, b, c \rightarrow (\alpha, \beta)$ is the Clarke transformation which produces a two coordinate time variant system.
- $\alpha, \beta \rightarrow d, q$ is the Park transformation which produces a two coordinate time invariant system.

3.2.1. The $(a, b, c) \Rightarrow (\alpha, \beta)$ Projection (Clarke Transformation)

Space vector projection can be represented by only two orthogonal axes called alpha and beta (α, β). Let suppose the axis a and the axis α are unidirectional as shown in the following vector diagram Figure III.2.

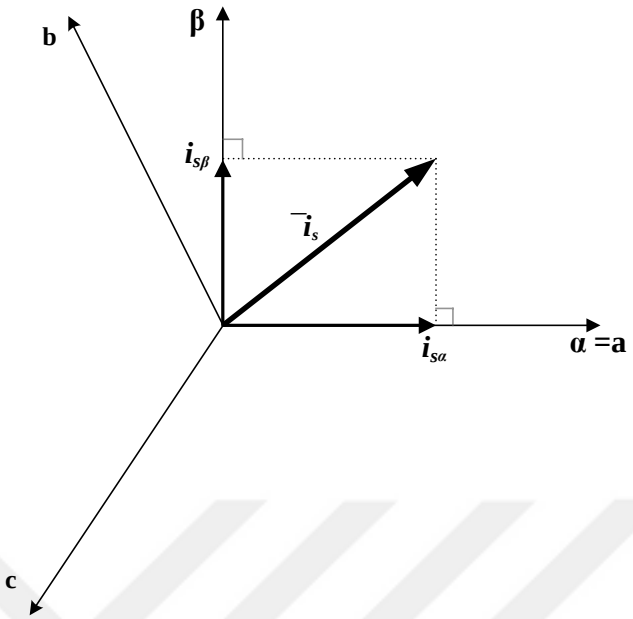

Figure III.2. Stator current space vectors and its components in the stationary reference frame.

The equations for projection of (α, β), the two-dimension orthogonal speed and time dependent system are:

$$i_{s\alpha} = i_a \tag{III.3}$$

$$i_{s\beta} = \frac{1}{\sqrt{3}} i_a + \frac{2}{\sqrt{3}} i_b. \tag{III.4}$$

3.2.2. The $(\alpha, \beta) \Rightarrow (d, q)$ Projection (Park Transformation)

This transformation is the most significant part of the FOC. This projection adapts a two phase orthogonal system (α, β) in the d–axis and q–axis rotating reference frame. Figure III.3 represents the relationship between the two reference frames when the rotor flux is aligned with the d–axis.

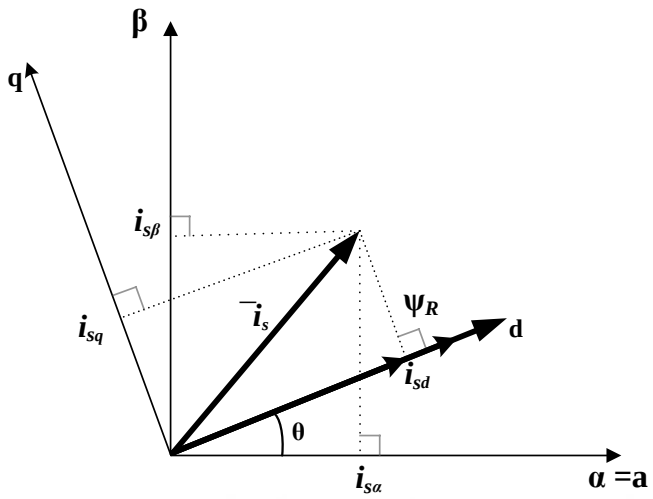

Figure III.3. Stator current space vectors and its components in (α, β) and in d–q rotating reference frame.

In Figure III.3, θ is the positon of rotor flux. The current vectors for torque and flux components are:

$$i_{sd} = i_{sa}\cos\theta + i_{s\beta}\ \sin\theta \tag{III.5}$$

$$i_{sq} = -i_{sa}\sin\theta + i_{s\beta}\ \cos\theta. \tag{III.6}$$

The above components depend on the components of current vector in (α, β) projection and the position of rotor flux. It is clear that if we knew the position of the rotor flux then the d–q component becomes a constant in this projection. Therefore, the two phase currents in (α, β) now turn into two DC quantities (time-independent). Now from here, controlling of torque is easy, and also i_{sq} (torque component) & i_{sd} (flux component) current components are independently controlled from here.

3.3. Dynamic Modeling of Induction Machine

In the area of design and implementation of ACI motor drives, dynamic modeling of induction machine is needed with controller design to control the parameters of the induction motor. The transient and steady state analysis will be considered in the dynamic model of IM. The mathematical model can be obtained from either transfer functions in s-domain or z-domain or state space equations or linear & non-linear differential equations [20]. Mathematical modeling is further utilized in designing of induction motor variable speed drives with variety of controllers like fuzzy logic controllers, PI controllers etc. Controller design depends on torque, flux and speed of the system. The mathematical modeling of induction machine discussed here is frequently utilized in machine dynamics, comprised of four voltage differential equations in terms of stator and rotor reference frames. The machine model is based on the d-q model of the induction machine with steady and transient state behaviors [21].

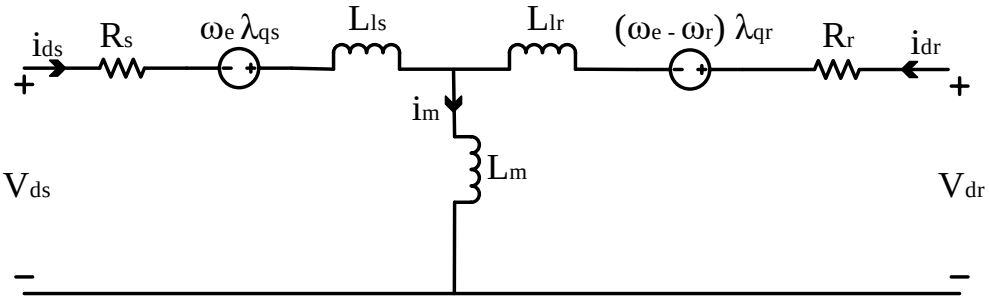

Figure III.4. d–axis equivalent circuit of induction motor.

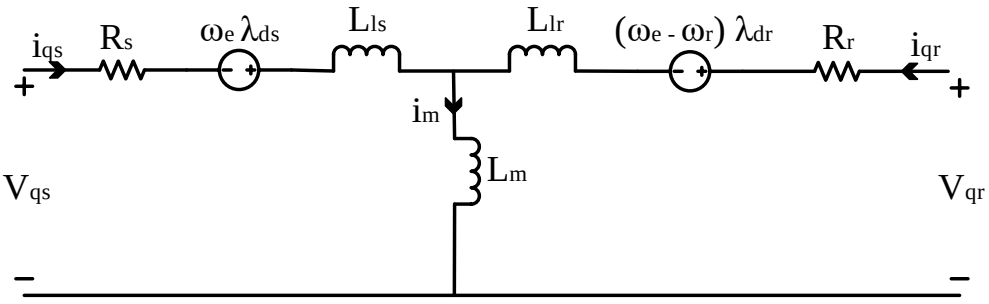

Figure III.5. q–axis equivalent circuit of induction motor.

The differential voltage equations by analyzing of the circuits from Figure III.4 and Figure III.5 are as follows:

$$V_{ds} = R_s i_{ds} + \frac{d\lambda_{ds}}{dt} - \omega_e \lambda_{qs} \tag{III.7}$$

$$V_{qs} = R_s i_{qs} + \frac{d\lambda_{qs}}{dt} - \omega_e \lambda_{ds} \tag{III.8}$$

$$V_{dr} = 0 = R_r i_{dr} + \frac{d\lambda_r}{dt} - (\omega_e - \omega_r)\lambda_{qr} \tag{III.9}$$

$$V_{qr} = 0 = R_r i_{qr} + \frac{d\lambda_{qr}}{dt} + \ \omega_e - \omega_r \ \lambda_{qr}. \tag{III.10}$$

The equations for flux linkages from (III.7) to (III.10) can be written as follows:

$$\lambda_{ds} = L_s i_{ds} + L_m i_{dr} \tag{III.11}$$

$$\lambda_{qs} = L_s i_{qs} + L_m i_{qr} \tag{III.12}$$

$$\lambda_{dr} = L_r i_{dr} + L_m i_{ds} \tag{III.13}$$

and

$$\lambda_{qr} = L_r i_{qr} + L_m i_{qs}. \tag{III.14}$$

From (III.11) to (III.14), the self-inductances can be expressed as:

$$L_s = L_m + L_{ls} \tag{III.15}$$

$$L_r = L_m + L_{lr}. \tag{III.16}$$

The equations for currents are obtained from (III.11) to (III.14) as:

$$i_{ds} = \frac{\lambda_{ds} - L_m i_{dr}}{L_s} \tag{III.17}$$

$$i_{qs} = \frac{\lambda_{qs} - L_m i_{qr}}{L_s} \tag{III.18}$$

$$i_{dr} = \frac{\lambda_{dr} - L_m i_{ds}}{L_r} \tag{III.19}$$

$$i_{qr} = \frac{\lambda_{qr} - L_m i_{qs}}{L_r}. \tag{III.20}$$

Now making the substitutions, so the current can be written at the end as follows;

Putting i_{dr} value in (III.17), we get

$$i_{ds} = \frac{\lambda_{ds} - L_m(\frac{\lambda_{dr} - L_m i_{ds}}{L_r})}{L_s}. \tag{III.21}$$

By calculating the above equation, we get the following equation

$$i_{ds} = \frac{L_r}{L_r L_s - L_m^2}\lambda_{ds} - \frac{L_m}{L_r L_s - L_m^2}\lambda_{dr}. \tag{III.22}$$

Putting i_{qr} value in (III.18), we get

$$i_{qs} = \frac{\lambda_{qs} - L_m(\frac{\lambda_{qr} - L_m i_{qs}}{L_r})}{L_s}. \tag{III.23}$$

By calculating the above equation, we get the following equation

$$i_{qs} = \frac{L_r}{L_r L_s - L_m^2}\lambda_{qs} - \frac{L_m}{L_r L_s - L_m^2}\lambda_{qr}. \tag{III.24}$$

Now putting i_{ds} value in (III.19), we get

$$i_{dr} = \frac{\lambda_{dr} - L_m(\frac{\lambda_{ds} - L_m i_{dr}}{L_s})}{L_r}. \tag{III.25}$$

Calculating the above equation, we get

$$i_{dr} = \frac{L_s}{L_r L_s - L_m^2}\lambda_{dr} - \frac{L_m}{L_r L_s - L_m^2}\lambda_{ds}. \tag{III.26}$$

To find i_{qr}, put i_{qs} value in (III.20), so we get the following equation:

$$i_{qr} = \frac{\lambda_{qr} - L_m(\frac{\lambda_{qs} - L_m i_{qr}}{L_s})}{L_r}. \tag{III.27}$$

By calculating equation (III.27), we get

$$i_{qr} = \frac{L_s}{L_r L_s - L_m^2}\lambda_{qr} - \frac{L_m}{L_r L_s - L_m^2}\lambda_{qs}. \tag{III.28}$$

The induction motor electromagnetic-torque can be written as:

$$T_e = \frac{3}{2} * \frac{P}{2} * L_m[i_{qs} i_{dr} - i_{ds} i_{qr}] \tag{III.29}$$

By neglecting the mechanical damping of the motor, the relation of torque and rotor speed are as:

$$\frac{d\omega_r}{d_t} = \frac{P}{2J}\ T_e - T_L\ . \tag{III.30}$$

By integrating the frequency of the input voltages, the angle θ_e can be calculated directly as:

$$\theta_e = \int_0^t \omega_e\, d_t + \theta_e(0) \tag{III.31}$$

where $\theta_e(0)$ is the initial rotor position.

The 3−ϕ voltages are converted to 2−ϕ stationary (s) reference frame using the following matrix equation:

$$\begin{bmatrix} V_{qs}^s \\ V_{ds}^s \end{bmatrix} = \begin{bmatrix} 1 & 0 & 0 \\ 0 & -\frac{1}{\sqrt{3}} & \frac{1}{\sqrt{3}} \end{bmatrix} \begin{bmatrix} V_{an} \\ V_{bn} \\ V_{cn} \end{bmatrix}. \tag{III.32}$$

The 2−ϕ stationary reference frame voltages can be converted to synchronously rotating reference frame by utilizing the following equations:

$$V_{qs} = V_{qs}^s \cos\theta_e - V_{ds}^s \sin\theta_e \tag{III.33}$$

and

$$V_{ds} = V_{qs}^s \sin\theta_e - V_{ds}^s \cos\theta_e. \tag{III.34}$$

The following equations are for finding the current variables i.e.

$$i_{qs}^{s} = i_{qs}\cos\theta_e + i_{ds}\sin\theta_e \tag{III.35}$$

and

$$i_{ds}^{s} = -\,i_{qs}\sin\theta_e + i_{ds}\cos\theta_e \tag{III.36}$$

and

$$\begin{bmatrix} i_a \\ i_b \\ i_c \end{bmatrix} = \begin{bmatrix} 1 & 0 \\ -\frac{1}{2} & -\frac{\sqrt{3}}{2} \\ -\frac{1}{2} & \frac{\sqrt{3}}{2} \end{bmatrix} \begin{bmatrix} i_{qs}^{s} \\ i_{ds}^{s} \end{bmatrix}. \tag{III.37}$$

3.3.1. Matlab/Simulink model equations

To build a dynamic model of the induction motor, the underneath four equations which are derived by substituting all the required variables in equations (III.7), (III.8), (III.9) and (III.10), producing the following differential equations which are written in the form of the flux linkages i.e.

$$\frac{d\lambda_{ds}}{dt} = V_{ds} - \frac{R_s L_r}{L_r L_s - L_m^2}\ \lambda_{ds} + \frac{R_s L_m}{L_r L_s - L_m^2}\lambda_{dr} - \omega_e \lambda_{qs} \tag{III.38}$$

$$\frac{d\lambda_{qs}}{dt} = V_{qs} - \frac{R_s L_r}{L_r L_s - L_m^2}\ \lambda_{qs} + \frac{R_s L_m}{L_r L_s - L_m^2}\lambda_{qr} - \omega_e \lambda_{ds} \tag{III.39}$$

$$\frac{d\lambda_{dr}}{dt} = -\frac{R_r L_s}{L_r L_s - L_m^2}\ \lambda_{dr} + \frac{R_r L_m}{L_r L_s - L_m^2}\lambda_{ds} - (\omega_e - \omega_r)\lambda_{qr} \tag{III.40}$$

and

$$\frac{d\lambda_{qr}}{dt} = -\frac{R_r L_s}{L_r L_s - L_m^2}\ \lambda_{qr} + \frac{R_r L_m}{L_r L_s - L_m^2}\lambda_{qs} -\ \ \omega_e - \omega_r\ \lambda_{dr}. \tag{III.41}$$

The Simulink mathematical model (Simulink blocks) can be constructed by creating subsystems while utilizing the equations i.e. (III.11) to (III.14), (III.15),(III.16), (III.22), (III.24), (III.26), (III.28), and (III.34) to (III.37). The overall Simulink dynamic model of the induction motor is shown in appendix section.

3.4. The Basic Procedure for the IFOC

Figure III.6 below first describes the measurement of two phase currents from the motor feed the Clarke transformation module. The Clarke module outputs i_α and i_β currents. Then i_α and i_β currents are the inputs to the park transformation module which then outputs the currents i.e. i_d and i_q in d–q rotating reference frame. After park transformation, i_d and i_q currents are compared to the flux reference (i_d^*) and the torque reference (i_q^*). Remember at this point, that this structure can either be used for asynchronous or synchronous motors just by altering the reference flux and getting the position of the rotor flux. The rotor flux is known and fixed by the magnets in synchronous motors. Hence, PMSM can be controlled by zeroing the value of i_d^*. On the other hand, induction motors need creation of a rotor flux for proper operation so the flux reference should not be zero. This relatively solve the issues of classic control schemes, the portability from asynchronous to synchronous machine drives. A current model block is used for completing Indirect FOC operation, because in IFOC proper angle (θ_e) is needed by park and inverse park transformation blocks for efficient operation. Current model needs i_d and i_q currents and speed (ω_m) from QEP as inputs and outputs the required angle (θ_e).

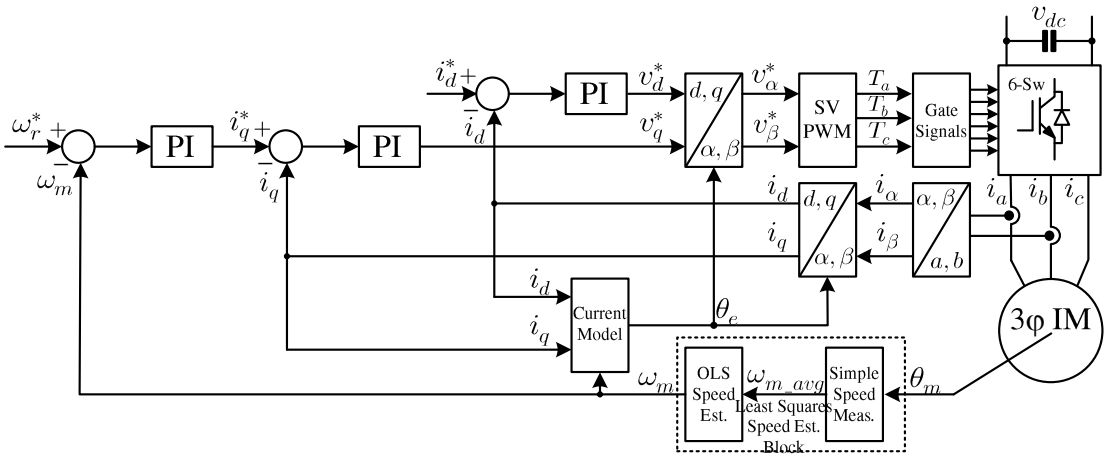

Figure III.6. Overall block diagram of Indirect FOC scheme of IM drive with low-count encoder using ordinary least squares (OLS) speed estimation.

During the speed IFOC, the torque command ($i_q{}^*$) is the output from the speed controller. Current regulator outputs are V_d^* and V_q^* which are then inputted to the inverse Park transformation. The IPark block will outputs V_α and V_β which are the parts of the stator vector voltage in the stationary orthogonal (α, β) frame of reference. V_α and V_β are feed in to the SVPWM (space vector pulse width modulation). The inverter is being driven by six modulated outputs from SVPWM block. Remember that both Park and IPark transformation blocks requires the position of the rotor flux depending on the type of AC machine (synchronous or asynchronous).

3.4.1. Position of Rotor Flux

The rotor flux position is the main component of IFOC of Induction motor [22]. Error will occur, if the rotor flux is not in-lined with d–axis. It means that i_q and i_d are then termed as incorrect torque and flux components of the stator current (i_s). Figure III.7 represents the current, voltage and rotor flux space vectors in the d, q rotating

reference frame and their relationship with a, b, c and (α, β) stationary reference frame [19].

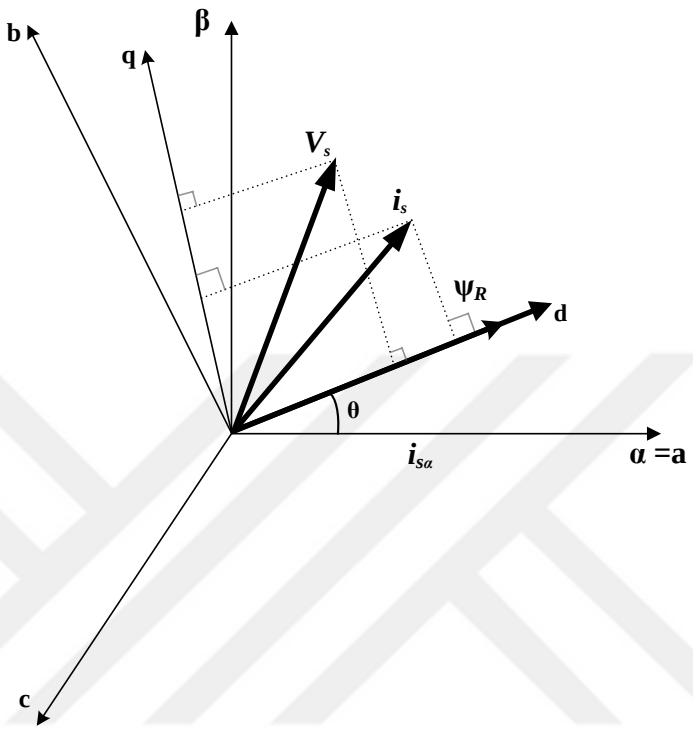

Figure III.7. Current, voltage and rotor flux space vectors in d-q rotating reference frame and their relationship with (a, b, c) and (α, β) stationary reference frame.

Synchronous and induction machines are different in a sense of the rotor flux position. i.e.

- In the synchronous machines, due to permanent magnets, the speed of the rotor is equal to the speed of rotor flux (means no slip). So, rotor flux position (θ) can easily be calculated by position sensor (e.g., hall sensors) or by the rotor speed integration.
- In the asynchronous machines, there are no magnets, so the speed of the rotor is not equal to the speed of rotor flux (because of the slip speed). Therefore, it requires

a particular method to measure rotor flux position (θ). For this purpose, we use current model by using two equations of the asynchronous (induction) motor model in d, q reference frame.

Theoretically, the field oriented control for the induction motor drive can be mainly divided into two types of schemes i.e. on the basis of the stator, rotor, or air gap flux linkages [22]:

i. **Indirect FOC**

   In the indirect field oriented control, the slip estimation with estimated rotor speed is needed for calculating the synchronous speed. There is no flux measurement in IFOC system.

ii. **Direct FOC**

   In the direct scheme, the synchronous speed is calculated from the flux angle which is accessible from flux estimator or flux sensors (e.g., Hall-effect sensors).

3.4.2. Current Model

The mechanical position sensor (QEP or tachometer) in asynchronous motors cannot measure position of rotor flux θ directly, because the angular speed between mechanical rotor and the rotor flux are not equal. For this purpose, 3–ϕ AC Induction motor in FOC control have been supplied with current model module in order to attain a speed and current closed loop system. Therefore, the system becomes IFOC (Indirect field oriented control) now. The current model comprised of the following two equations in d, q reference frame.

$$i_{dS} = T_R \frac{di_{mR}}{dt} + i_{mR} \tag{III.42}$$

$$f_S = \frac{1}{\omega_b}\frac{d\theta}{dt} = n + \frac{i_{qS}}{T_R i_{mR} \omega_b}. \tag{III.43}$$

where, θ is the rotor flux position.

i_{mR} is the magnetizing current.

$T_R = \frac{L_R}{R_R}$ is the rotor time constant with L_R the rotor inductance and R_R the rotor resistance.

f_S is the rotor flux speed, and

ω_b is the electrical nominal flux speed.

Remember, it is necessary to know about rotor time constant because the correct functioning of current model can only be achieved by integration of the rotor flux position through the rotor flux speed outputs.

IV. BASIC SPEED & POSITION ESTIMATION METHODS

Most of the control algorithms are based on the measurement of speed, position and acceleration. Variable speed drive performances are improved often by using position and speed feedback. In today's era, instead of rotor speed measurement, many of methods are used and available for rotor speed estimations with the main advantage of reducing mathematical calculations while maintaining high accuracy. Famous ones are adaptive filters, artificial intelligent techniques, frequency signal injection techniques, different observers such as Kalman, sliding mode, Luenberger in low and high speeds. But most of them require high mathematical computations. A direct torque control of surface mounted PMSM is presented in [23] for finding a solution to the agitation part of a washing machine by estimation of torque and speed with low cost hall-effect sensors for constant torque region. Some of the basic concepts and methods used for speed measurements and estimations are discussed here below, relating to the novel method used in this project for speed measurement from position information which will be discussed later.

4.1. Classical Method

The rotating optical encoder produce two square waves in quadrature with 90º phase difference. In both waves, the transition is detected as the encoder line. The position measurement error depends on the number of output pulses in each revolution. The maximum error in the instantaneous position is:

$$\Delta\theta = \frac{2\pi}{N} \tag{IV.1}$$

where N represents the number of pulses per revolution of encoder. The discrete speed is obtained from the discrete position as:

$$\Omega_k = \frac{\theta_{\ k} - \theta_{k-1}}{T_v} \tag{IV.2}$$

where T_v is the sampling period of speed.

By using the Taylors first order series expansion of the position, result is obtained and thus absolute error of speed can be written as:

$$\Delta\Omega = \frac{2\Delta\theta}{T_v} = \frac{4\pi}{N\ T_v}. \tag{IV.3}$$

The error and sampling period are inversely proportional to each other. The sampling period must be set such that the error does not increase much, so that linear approximation is valid. As a result, the speed estimation is different than the real speed for sure. Note that if control algorithm requires acceleration, then the absolute error will be more affected by T_v as shown in the equation of absolute acceleration below [24].

The equation of discrete acceleration is:

$$\Omega_k = \frac{\Omega_k - \Omega_{k-1}}{T_v}. \tag{IV.4}$$

Therefore, absolute acceleration error will be:

$$\Delta\Omega = \frac{2\Delta\Omega}{T_v} = \frac{8\pi}{N\ T_v^2}. \tag{IV.5}$$

Means with decreasing of sampling period, this acceleration increases very rapidly. Result for speed estimation of a DC motor with $T_v = 4.8$ ms using the classical method is shown in Figure IV.1.

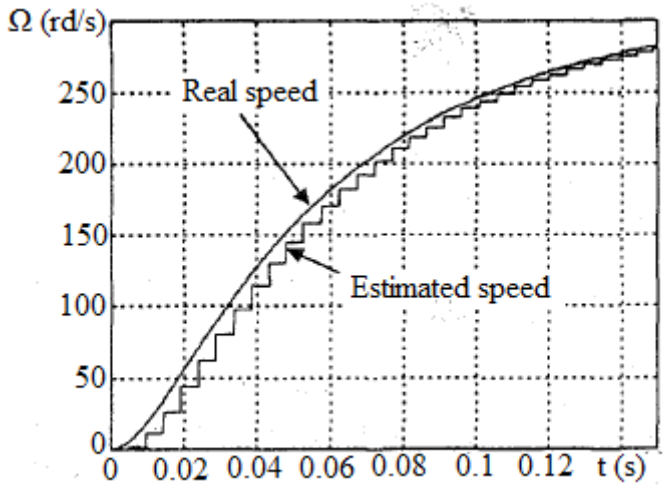

Figure IV.1. Classical speed estimation method of a DC motor ($T_v = 4.8$ ms) [24]

4.2. Least Square Method

The linear least square method (LSM) is a very widely used popular technique used in statistics. This is one of the oldest methods which was first published by a French mathematician Legendre in 1805, but a very famous German mathematician, Gauss published this method in 1809 and claimed that he discovered and used this LSM in 1795 earlier than Legendre. Therefore, a priority dispute is there but anyhow it did not decline the popularity of this method.

Nowadays, least square method is more widely used in estimation of the numerical values of parameters of a set of data to fit a function (example, linear regression) and also characterizing the statistical properties of the estimates. LSM is used in several varieties such as ordinary least squares (OLS), which is a simpler type and a more advanced version called weighted least squares (WLS), which has better performance

than the ordinary one. Some recently used varieties of least square method are partial least squares (PLS) and alternating least squares (ALS).

In [24], several equations are computed based on standard least square technique by estimating the speed from position information and comparing the estimated speed with the real speed of the DC motor. This estimated speed performance is better than that of the classical method. The advantage of LSM is the mathematical operations are reduced as compared to other methods.

4.3. Frequency & Period Measurement Methods

The resolutions of encoders used for position and speed estimations and measurements heavily affects the accuracy, bandwidth and cost of the drive system. The two pulse trains from the encoder calculates the actual rotor position and speed which is required for motor control. If the encoders are low count, it will definitely have some error. So to overcome these limitations, there are some novels for speed calculation algorithms introduced in [25] based on the direct measurement of the period and frequency of the quadrature signals from encoder. In [26], commonly used procedures are proposed for speed estimation: the period measurement method at low speed and frequency measurement method for high speeds. It discusses the errors occurs in these methods and also proposed a solution for good performance at low resolutions. Note that the frequency measurement method is only suitable at high speeds while the period measurement method is used and works fine with low speeds.

4.3.1. Frequency Measurement Method

In order to estimate the speed from the output signal of the encoder, fixed time period is used by measuring the output number of pulses which are generated from the

encoder. This method is called the frequency measurement method proposed in [25], [26] and [27]. It is only suitable for high speed ranges where the number of pulses ΔN coming from the encoder in a fixed sampling time T_s is higher. The error is inversely proportional to speed means at low speeds, the error will be high just because of the small number of encoder pulses in a fixed sampling time as shown in Figure IV.2. from [26]. the expression for the angular speed is:

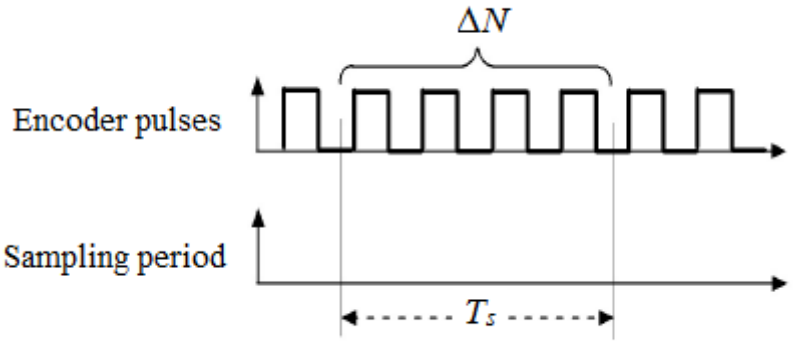

Figure IV.2. Speed estimation based on the frequency measurement method.

$$\omega_f = \frac{d\theta}{dt} \cong \frac{d\theta}{T_s} \cong \frac{2\pi\Delta N}{N_r T_s} = \frac{\theta_p \Delta N}{T_s}. \tag{IV.6}$$

In above equation, N_r is the number of pulses per revolution. The quantization error which occurs in this method is due to the lack of synchronization between the observation window and the encoder pulses.

Quantization error of the speed measurement is calculated as:

$$\Delta\omega_f = \frac{2\pi}{N_r T_s}. \tag{IV.7}$$

At high speeds, the frequency measurement method produce small errors, because the main reason is the number of pulses in the specific time interval is high.

4.3.2. Period Measurement Method

This method is evaluated by counting the number of pulses during two consecutive encoder pulses of a high frequency clock signal [25], [26]. Figure IV.3 shows the principle of this method in which n is the number of high frequency pulses with having a period T_{hf}.

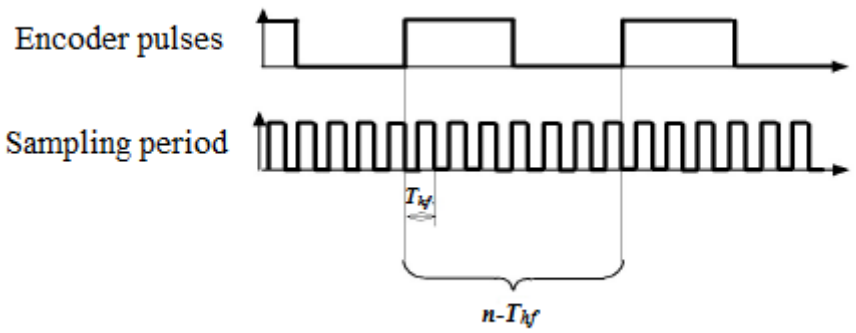

Figure IV.3. Speed estimation based on the period measurement method.

The expression for angular speed is:

$$\omega_p = \frac{d\theta}{dt} \cong \frac{d\theta}{nT_{hf}} \cong \frac{2\pi}{N_r nT_{hf}} \tag{IV.8}$$

The speed estimation based on this method at low speed produces relatively small errors due to the high frequency pulses during two consecutive encoder pulses. Error is higher at high speed due to the small number of high frequency pulses during two consecutive pulses.

V. METHODOLOGY

In the next sections, an ordinary least squares (OLS) speed estimation algorithm (linear and quadratic) is used to achieve better speed performance at very low speed by using low-count encoders. In this method, predetermined numbers of speed data sets are best fit by both linear and quadratic least squares algorithms such that more realistic speed results can be achieved. Simulation tests will show that when OLS speed estimation is used quite satisfactory speed responds are observed. These results will be experimentally validated to illustrate the superiority of the OLS speed estimation on low speed performance for IFOC of PMSM drive by using the low-count encoders compared to the common techniques explained fully in later chapters.

5.1. Low Speed Measurement Using Low-Count Encoder

In indirect field oriented control (IFOC) of IM drive, in or-der to find the rotor flux position, it is necessary to measure the rotor mechanical speed. Usually, incremental encoder is preferred as speed and position sensor in speed controlled drive systems. It has two outputs and produces 90-degree phase shifted two pulse trains with respect to each other and period of pulses vary proportional to the rotor speed. The two output channels (A and B) of sensor can be connected directly to the QEP & CAP units of the DSP controller TMS320F28335, which counts both edges of the pulses. A 1024 pulse incremental encoder is used to measure the motor speed. Simple algorithms are developed to try different pulse resolution which down samples the number of 1024 pulses to any low-count encoder resolution. In this work, 1024 pulses were down sampled to 32, 16, 8, and 4 pulse encoder feedback to test the overall system like a low pulse encoder. Using this property, the accuracy of the speed measurement and the

performance of the FOC are tested with different pulse encoder outputs. The low speed performance during start-up and two quadrant operation with each low-count encoders are experimentally investigated first by using common method such that keeping the previous sampled-speed constant throughout the present interval of the low-count encoder pulses and later by OLS speed estimation method for possible comparison of both methods [11].

Since a low-count encoder does not have enough resolution at low speeds, the simple speed control system exploits a method which is based on the measurement of time between the two encoder pulses and has upper limit restriction due to the switching frequency limit of IGBTs. Appropriate resolution of the low speed region is under 0.1 pu. Although the low speed can be measured effectively with CAP units of 283xx, the direction of the speed cannot be identified. In most of the applications, the machine is operated in the two quadrant motoring regions. Therefore, the direction of the speed should be known. The direction of the speed is sensed by QEP units and fed back to low speed module. Since CAP and QEP use different timers and event managers, their operations do not interrupt each other [11].

Another problem associated in this project is the counter overflows. Since the timers of TMS320F28335 count quite fast even with the highest prescalar, the low speed detection algorithm collapses during low speeds range due to counter overflows. Therefore, a simple overflow detecting and counting algorithm is added to speed detection module to sense the very low speed with high precision.

5.2. Ordinary Least Square (OLS) Speed Estimation Method

The least squares method, a very popular technique, is frequently used to compute estimations of parameters and to fit data. It is one of the oldest techniques of modern

statistics dis-covered in the late 1700s and the beginning of 1800s. Since then, the popularity of the least square method is not diminished. It is widely used in many areas including electrical engineering to find or estimate the numerical values of parameters of estimates such as sensorless control of motor drives and parameter estimation of electrical machines. There are several variations of this method: the simplest is the ordinary least squares (OLS) which is the subject of this paper, a more sophisticated version is called weighted least squares (WLS), and recently the alternating least squares (ALS) and partial least squares (PLS). Ordinary least squares estimation can be divided into two categories: linear and quadratic [6].

Linear least squares estimation corresponds to the problem of finding a line that best fits a set of data. A set of predetermined N pairs of observations {(X_1, Y_1), (X_2, Y_2), (X_3, Y_3), … (X_N, Y_N)} = { X_i, Y_i} = {$time$, $speed$} is used to find a function giving the value of the dependent variable (Y) corresponding to the measured speed from the values of an independent variable (X) which represents time in this case. Linear predicted function [28] from the collected sets of data can be represented by the following equation:

$$Y = a + bX \tag{V.1}$$

where a is the intercept and b corresponds to the slope of the regression line.

Least squares method involves minimizing the sum of the squares of the differences of measured Y_i and estimated (Y_i) data. It is therefore known as the least squares technique. The minimization expression is given by:

$$\varepsilon = \sum_{i=1}^{N}(Y_i - Y_i)^2 = \sum_{i=1}^{N}[Y_i - (a + bX_i)]^2 \tag{V.2}$$

where ε stands for "error" which is the quantity to be minimized. This is achieved by using standard techniques such that the quadratic (i.e. with a square) formula reaches its minimum value when its derivative vanishes. If the function depends on more than one variable as in the case of our example, the global minimum occurs when the derivative with respect to each of the variables (a and b) is zero. Followings are the sets of equations to find the parameters a and b:

$$\frac{\partial \varepsilon}{\partial a} = 2Na + 2b\sum_{i=1}^{N} X_i - 2\sum_{i=1}^{N} Y_i = 0 \tag{V.3}$$

and

$$\frac{\partial \varepsilon}{\partial b} = 2b\sum_{i=1}^{N} X_i^2 + 2a\sum_{i=1}^{N} Y_i - 2\sum_{i=1}^{N} Y_i\, X_i = 0 \tag{V.4}$$

where N is the number of sets of data.

From (V.3) the variable a can be solved and replaced in (V.4) to find the variable b. Finally, a and b can be obtained as follows:

$$a = \frac{\sum_{i=1}^{N} Y_i}{\mathrm{N}} - \mathrm{b}\frac{\sum_{i=1}^{N} X_i}{\mathrm{N}} = M_y - bM_x \tag{V.5}$$

$$b = \frac{\sum_{i=1}^{N} Y_i X_i - M_y \sum_{i=1}^{N} X_i}{\sum_{i=1}^{N} X_i^2 - M_x \sum_{i=1}^{N} X_i} \tag{V.6}$$

where My and Mx denote the mean values of Y and X, respectively.

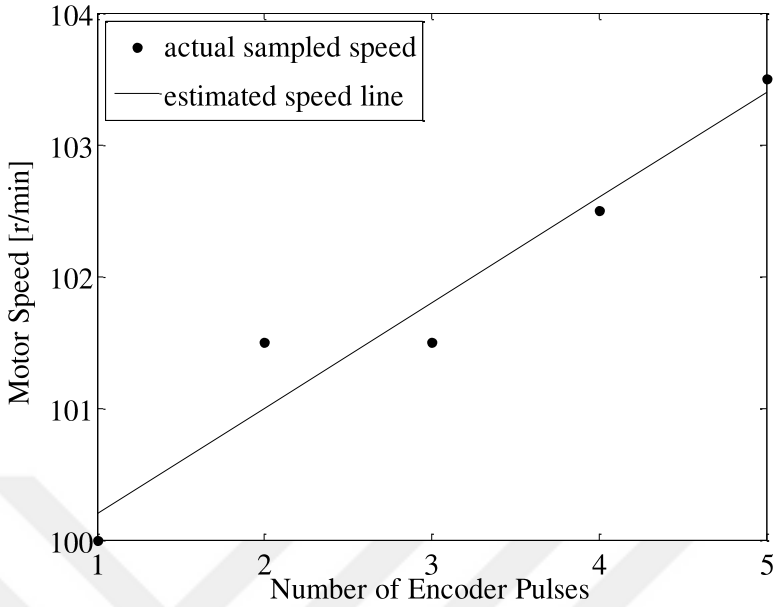

Figure V.1. Simulation of the linear least squares-based speed estimation.

In Figure V.1, the last five sampled rotor speeds are best fit by using linear least squares estimation technique explained above. The line in that figure is constituted as intercept a which is 99.4 and slope b as 0.8. The line is obtained by considering the predetermined number of speed data sets which is chosen as five in the above figure. After collecting and figuring out the speed line with five sampled data, obtained line is kept as it is until the next speed sample is read which depends on the number of encoder pulses and the speed of the rotor. When the next speed is measured, it is taken as the fifth data and the very first sampled of the last five speed data is eliminated, therefore new five sets of speed data are created to adjust the estimated speed line. Simple speed measurement method discussed above is still considered to calculate the speed when

the encoder pulse is read, but between intervals of the encoder pulses, OLS estimation is used.

There may be some cases that linear fitting is not suitable such as fluctuations in the motor speed due to the load torque distortions and curved/nonlinear speed references. Thus, quadratic least squares estimation has the benefit to fit the data in a nonlinear way. The general equation of a quadratic function has three variables and is given by:

$$Y = aX^2 + bX + c \tag{V.7}$$

where Y is the estimated quantity $(speed)$ and a, b, and c represent the variables of the quadratic equation.

To minimize the quadratic equation, the error function can be defined as follows:

$$\varepsilon = \sum_{i=1}^{N} (Y_i - Y_i)^2 = \sum_{i=1}^{N} [Y_i - \ aX_i^2 + bX_i + c \ ]^2 \tag{V.8}$$

where Yi denotes the measured quantity $(speed)$ and N is the number of sets of data $(\{time, speed\})$.

As in the linear least squares estimation the derivatives of the error function with respect to the variables a, b, and c set to zero to minimize the difference of the measured and estimated data $(speed)$ as follows:

$$\frac{\partial \varepsilon}{\partial a} = \sum_{i=1}^{N} [Y_i X_i^2 - (\ aX_i^4 + bX_i^3 + cX_i^2)] = 0 \tag{V.9}$$

and for b:

$$\frac{\partial \varepsilon}{\partial b} = \sum_{i=1}^{N} [Y_i X_i - (\ aX_i^3 + bX_i^2 + cX_i)] = 0 \tag{V.10}$$

and for c:

$$\frac{\partial \varepsilon}{\partial c} = \sum_{i=1}^{N} [Y_i - (aX_i^2 + bX_i + c)] = 0. \tag{V.11}$$

If (V.9–(V.11) are rewritten such that the terms that have Y_i in them appear on one side of the equation and the terms that do not are on the other side the following equations are obtained:

$$\sum_{i=1}^{N} Y_i X_i^2 = a \sum_{i=1}^{N} X_i^4 + b \sum_{i=1}^{N} X_i^3 + c \sum_{i=1}^{N} X_i^2 \tag{V.12}$$

$$\sum_{i=1}^{N} Y_i X_i = a \sum_{i=1}^{N} X_i^3 + b \sum_{i=1}^{N} X_i^2 + c \sum_{i=1}^{N} X_i \tag{V.13}$$

$$\sum_{i=1}^{N} Y_i = a \sum_{i=1}^{N} X_i^2 + b \sum_{i=1}^{N} X_i + Nc. \tag{V.14}$$

For convenience, each of the above equations (V.12–(V.14) consists the summations without the parameters a, b, and c can be defined as

$$z_1 = \sum_{i=1}^{N} X_i, z_2 = \sum_{i=1}^{N} X_i^2, z_3 = \sum_{i=1}^{N} X_i^3 , z_4 = \sum_{i=1}^{N} X_i^4 \tag{V.15}$$

$$w_1 = \sum_{i=1}^{N} Y_i, w_2 = \sum_{i=1}^{N} Y_i X_i, w_3 = \sum_{i=1}^{N} Y_i X_i^2. \tag{V.16}$$

Once the above equations replaced in (V.12–(V.14) the followings are obtained

$$w_1 = Nc + z_1 b + z_2 a \tag{V.17}$$

$$w_2 = z_1 c + z_2 b + z_3 a \tag{V.18}$$

$$w_3 = z_2 c + z_3 b + z_4 a. \tag{V.19}$$

To solve the variables a, b, and c above equations(V.17(V.19) can be formed as a 3x3 matrix called K, a (3x1) right hand side vector r, and a (3x1) solution vector s:

$$K = \begin{bmatrix} N & z_1 & z_2 \\ z_1 & z_2 & z_3 \\ z_2 & z_3 & z_4 \end{bmatrix}, r = \begin{bmatrix} w_1 \\ w_2 \\ w_3 \end{bmatrix}, s = \begin{bmatrix} c \\ b \\ a \end{bmatrix}. \tag{V.20}$$

The solution to the quadratic least squares problem is as a result, the vector s therefore the desired parameters can be found as [29]:

$$\begin{bmatrix} c \\ b \\ a \end{bmatrix} \quad \begin{bmatrix} D^{-1}[\ z_2 z_4 - z_3^2\ w_1 + \ z_2 z_3 - z_1 z_4\ w_2 + \ z_1 z_3 - z_2^2\ w_3] \\ D^{-1}[\ z_2 z_3 - z_1 z_4\ w_1 + \ N z_4 - z_2^2\ w_2 + \ z_1 z_2 - N z_3\ w_3] \\ D^{-1}[\ z_1 z_3 - z_2^2\ w_1 + \ z_1 z_2 - N z_3\ w_2 + \ N z_2 - z_1^2\ w_3] \end{bmatrix} \tag{V.21}$$

where D^{-1} is the inverse determinant of the matrix K.

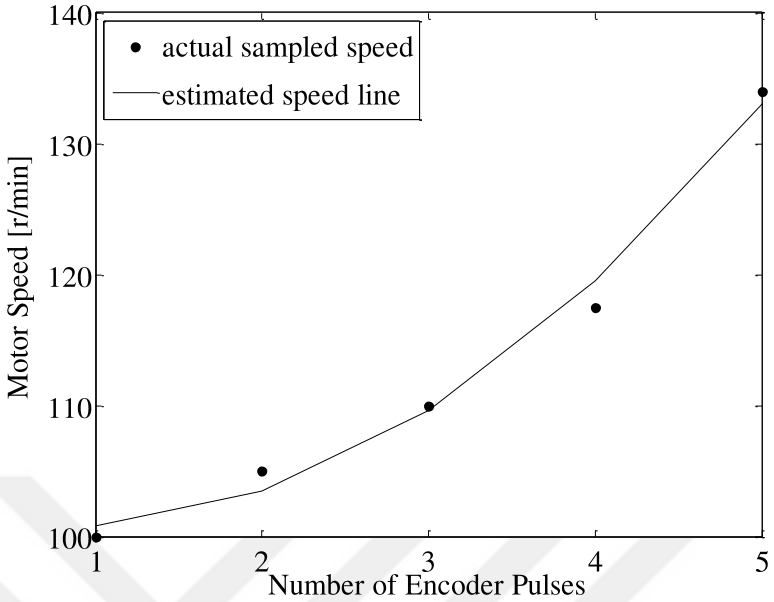

Figure V.2. Simulation of the quadratic least squares based speed estimation.

In some cases, linear least squares cannot provide good speed estimation such as when the motor speeds up not linearly but in a non-linear and curvy way. Figure V.2 depicts the simulated quadratic least squares speed estimation. In that example, five data corresponding speed versus encoder pulses are obtained. Then, by using (V.21) the necessary parameters for quadratic equation are found as: $a = 1.7857$, $b = 2.6143$ and $c = 101.6$. The same curve which is used to determine the estimated speed is fed back to the overall control system until the next encoder pulse is received. Once the data from the next pulse is obtained which is counted as the fifth point in the five sets of speed data, the first point in the data stream is discarded while the rest of the four data points are shifted down. As a result, with the new five sets of speed data, new values of the parameters (a, b, and c) can easily be found by using (V.21). Therefore, the quadratic equation is updated to be used as a speed feedback throughout the present position interval.

VI. EXPERIMENTAL RESULTS

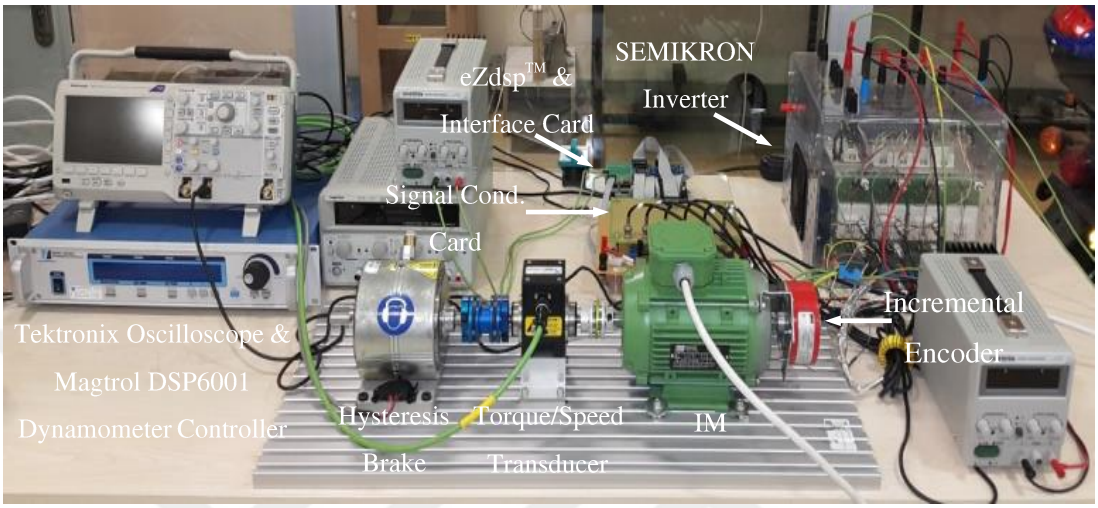

Figure VI.1. Experimental test-bed (top) Dynamometer controller, inverter, DSP control unit, interface and signal-conditioning cards, (bottom) IM with 1024 pulse incremental position encoder coupled to hysteresis brake through torque/speed transducer.

The feasibility and practical features of the simple and OLS based speed control schemes have been evaluated using an experimental test-bed, as shown in Figure VI.1. The proposed control algorithm is digitally implemented using the eZdsp™ board from Spectrum Digital, Inc. based on a 32-bit floating-point, 150 MHz digital signal processor TMS320F28335. A 4–pole, 1 hp induction motor setup shown in the bottom part of Figure VI.1, is driven by a custom designed SEMIKRON Semiteach PWM voltage-source inverter (VSI) which comprises SKM 50GB 123D model IGBT modules, SKHI 22 model gate drivers with 4.3 μs dead-time, and two 2200 μF caps., as shown in the top part of Figure VI.1. The induction motor is loaded with a Magtrol hysteresis dynamometer set contains 6 N·m hysteresis brake, a DSP6001 model

programmable DSP torque controller, and a Magtrol TMS306 model torque transducer to monitor the load torque and shaft speed which is installed between hysteresis brake and the motor, as shown in the bottom part of Figure VI.1. A 1024 pulse optical speed encoder is used to obtain low-count pulse by software modification.

In order to observe and compare the low speed performance of IFOC of IM drive using different encoders, the experiments are implemented under high resolution and low resolution speed feedback cases. Since the project is focused on low speed operation using a low-count encoder, the results are obtained which show the operation of motor where speed is less than the nominal value.

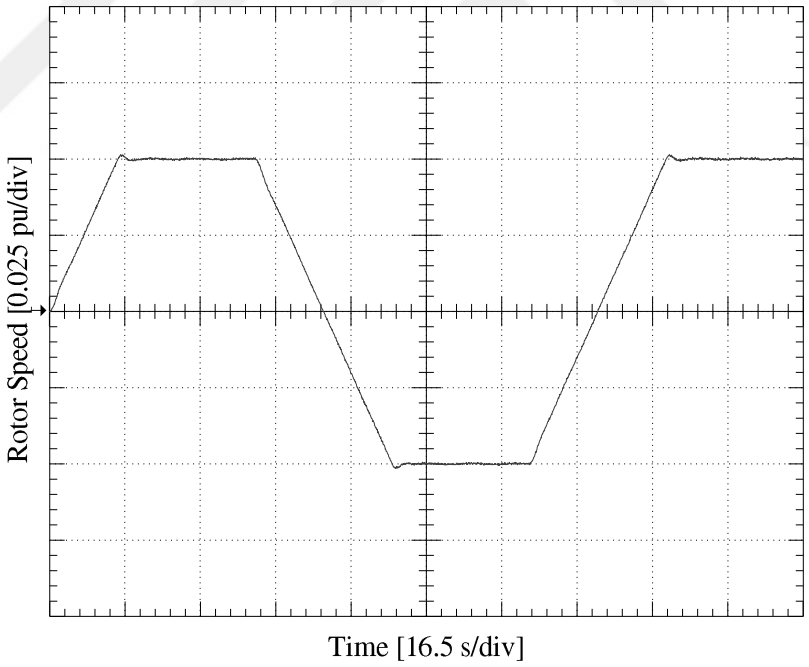

Figure VI.2. IFOC of IM performance for four-quadrant start-up and speed reversals (0 Hz to ± 2.5 Hz) using simple speed measurement technique with 1024 pulse encoder without OLS speed estimation (1 pu = 1500 r/min = 50 Hz).

First, the four quadrant speed reversal tests including no load start-up ramp performance in 15 seconds are done by using the simple speed measurement method which keeps the rotor speed constant during last interval of encoder pulses from 0 Hz to ± 2.5 Hz (± 0.05 pu = 75 r/min). As shown in Figure VI.3, Figure VI.4 and Figure VI.5, IFOC with low-count encoders has acceptable performance at near-zero speed transients where instability is encountered frequently. It is observed that the start-up transient can be achieved quite successfully even with four pulse encoder except at the very beginning and near zero speed due to the insufficient rotor position signal and simple speed measurement method. The flux reference component i_d^* is kept constant at 0.1 pu. The stability is established and the difference between the low-count encoders and 1024 (Figure VI.2) pulse encoder is acceptable.

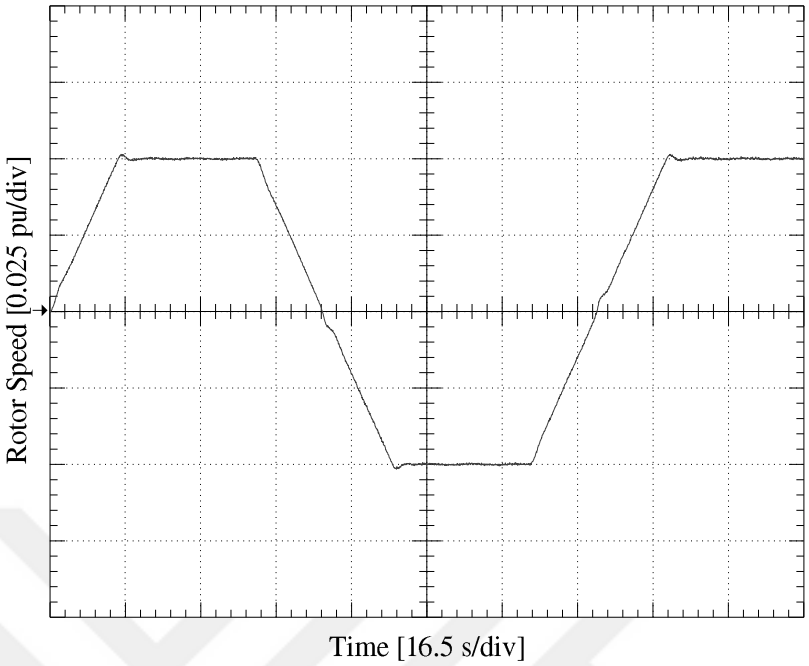

Figure VI.3. IFOC of IM performance for four-quadrant start-up and speed reversals (0 Hz to ± 2.5 Hz) using simple speed measurement technique with 16 pulse encoder without OLS speed estimation (1 pu = 1500 r/min = 50 Hz).

By using the least squares technique, the speed fluctuations observed at near-zero speed as shown in Figure VI.4 and Figure VI.5, where very low count encoder pulse signals (e.g. 4 and 8 pulse) used are claimed to be minimized. As it is seen in Figure VI.5, the worst case scenario happens with four pulse encoder near zero speed.

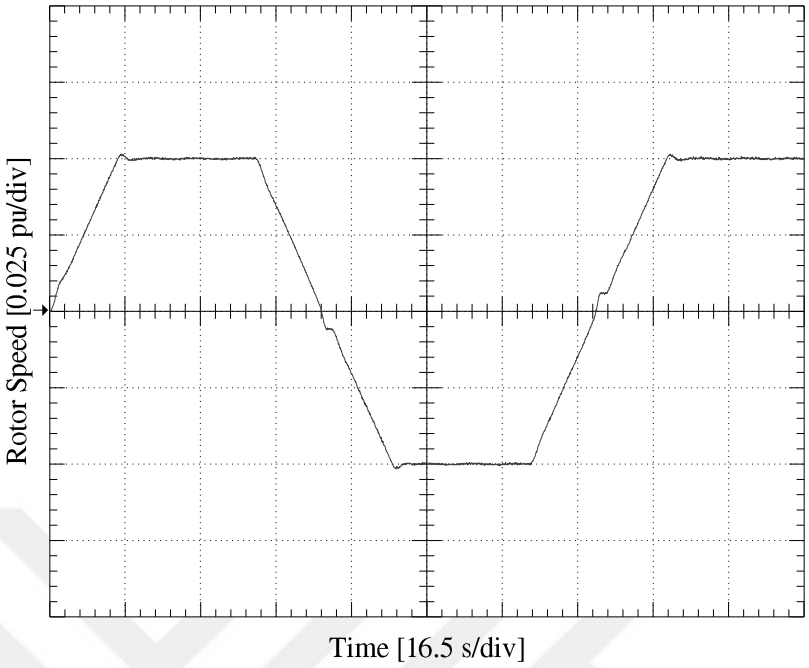

Figure VI.4. IFOC of IM performance for four-quadrant start-up and speed reversals (0 Hz to ± 2.5 Hz) using simple speed measurement technique with 8 pulse encoder without OLS speed estimation (1 pu = 1500 r/min = 50 Hz).

The rotor position is obtained by IFOC current model at every sampling period. Especially, when the speed is near zero speed regions very few encoder pulses are read, therefore sluggish speed estimation is inevitable.

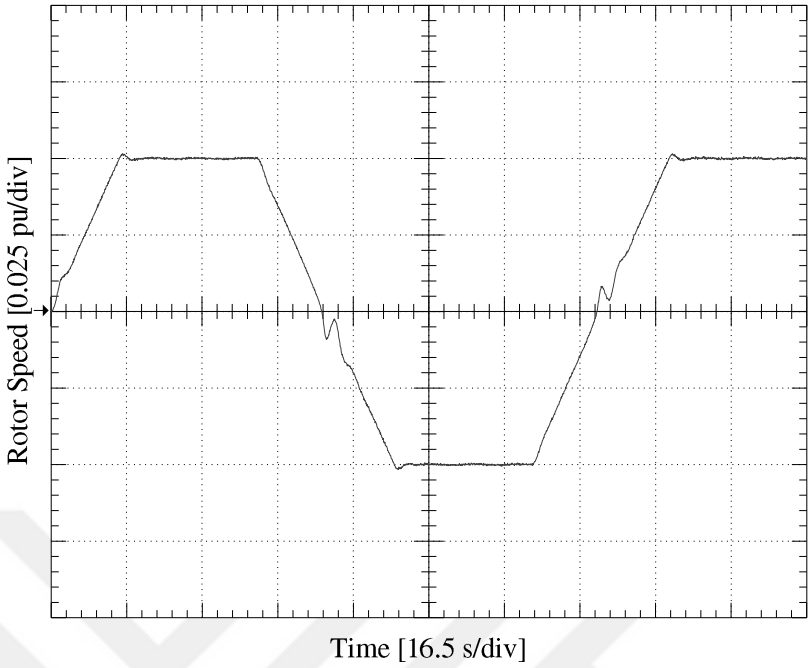

Figure VI.5. IFOC of IM performance for four-quadrant start-up and speed reversals (0 Hz to ± 2.5 Hz) using simple speed measurement technique with 4 pulse encoder without OLS speed estimation (1 pu = 1500 r/min = 50 Hz).

On the other hand, when OLS speed estimation is adopted as an estimation method, the data taken in the beginning of the four quadrant operation (0 Hz in Figure VI.2 to Figure VI.5) until the present time will be counted to determine the speed line and eventually more realistic speed can be obtained, as shown in Figure VI.6 to Figure VI.8.

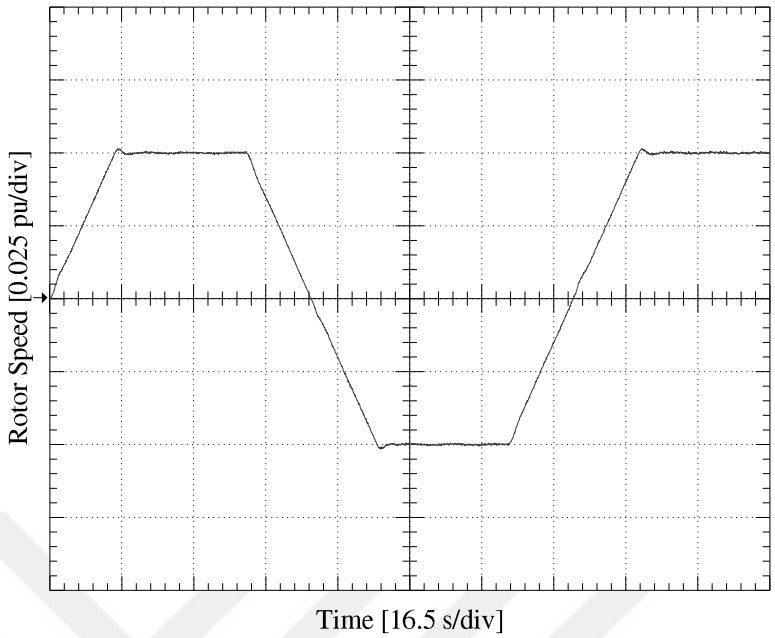

Figure VI.6. IFOC of IM performance for four-quadrant start-up and speed reversals (0 Hz to ± 2.5 Hz) with 16 pulse encoder using OLS speed estimation (1 pu = 1500 r/min = 50 Hz).

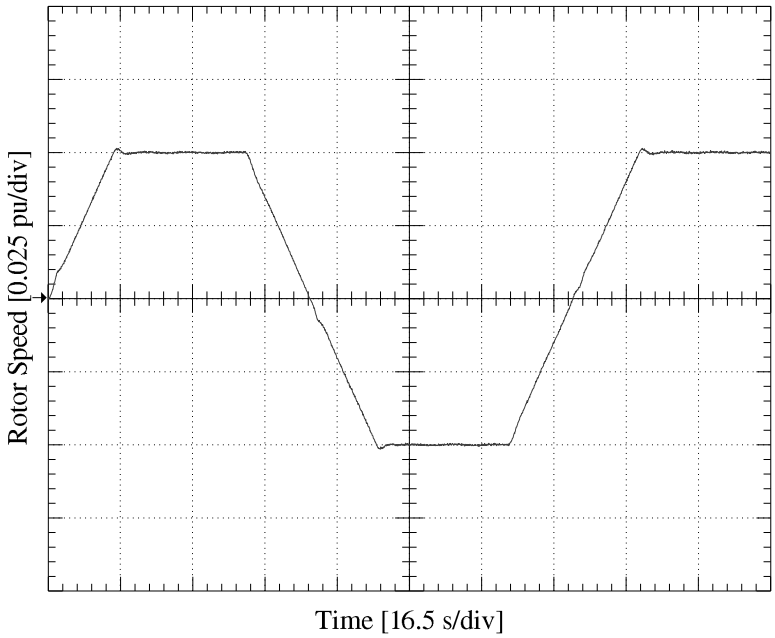

Figure VI.7. IFOC of IM performance for four-quadrant start-up and speed reversals (0 Hz to ± 2.5 Hz) with 8 pulse encoder using OLS speed estimation (1 pu = 1500 r/min = 50 Hz).

After first few data (N= predetermined numbers of data set), the line should be formed and from that moment at every position update of the new speed line is obtained such that the very first point in the data stream is discarded. Remaining ($N-1$) old data are shifted down and the new speed data is used as the last point of the data stream to form the N points. Then, necessary parameters in OLS (linear or quadratic) equation can be easily calculated to obtain the new speed line. Similarly, the four quadrant speed reversal tests including no load start-up with 15 seconds ramp performance are also performed by using OLS (linear) method from 0 Hz to ± 2.5 Hz (± 0.05 pu = 75 r/min).

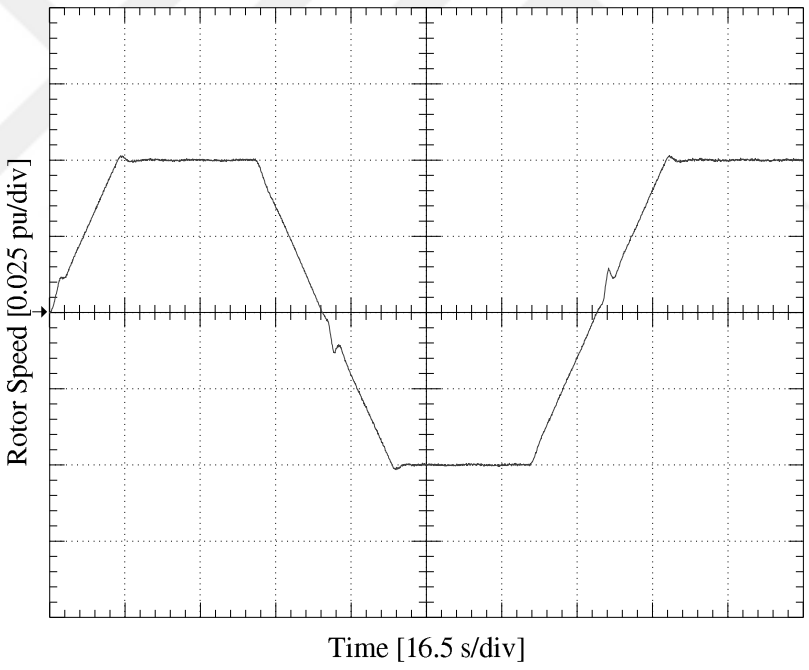

Figure VI.8. IFOC of IM performance for four-quadrant start-up and speed reversals (0 Hz to ± 2.5 Hz) with 4 pulse encoder using OLS speed estimation (1 pu = 1500 r/min = 50 Hz).

It is observed from Figure VI.6, Figure VI.7, and Figure VI.8, that the start-up transient and especially near zero speed performance can be improved successfully

even with four pulse encoder irrespective of the insufficient rotor position signal due to the help of OLS speed estimation compared to simple speed measurement method. The difference between the low-count encoders and 1024 pulse encoder is considerably small when OLS speed estimation is used. There exist small bumps in speed wave-forms at every zero crossing especially with four pulse encoder due to insufficient number of encoder pulses and high moment of inertia of the overall system. The higher the encoder pulse numbers, the lower the bumps are.

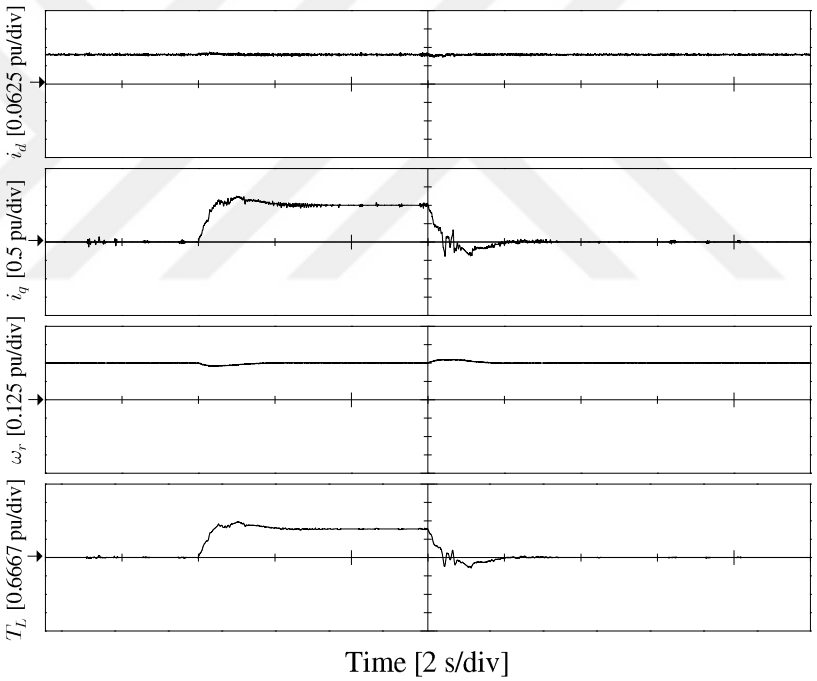

Figure VI.9. IFOC of IM performance under full load at 12.5 Hz (375 r/min) with 16 pulse encoder using OLS speed estimation.

At steady state, a step full load and half load are injected at $t = 4$ s and rejected at $t = 12$ s, as shown in Figure VI.9, Figure VI.10, Figure VI.11 and in Figure VI.12, Figure VI.13, and Figure VI.14, respectively. During the load tests, the flux reference

component i_d^* is kept constant at 0.1 pu. The stability is achieved during steady-state and transient load tests even with very low encoder pulses when OLS is performed.

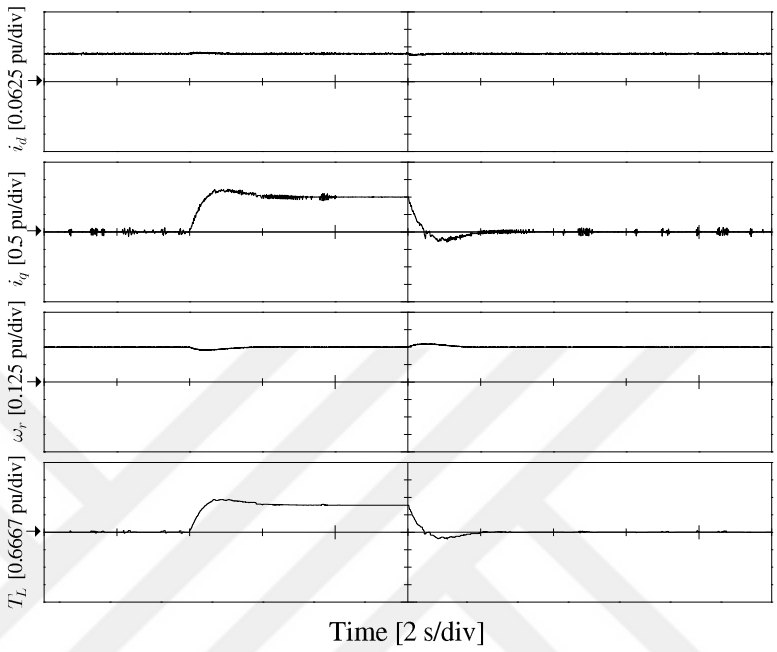

Figure VI.10. IFOC of IM performance under full load at 12.5 Hz (375 r/min) with 8 pulse encoder using OLS speed estimation.

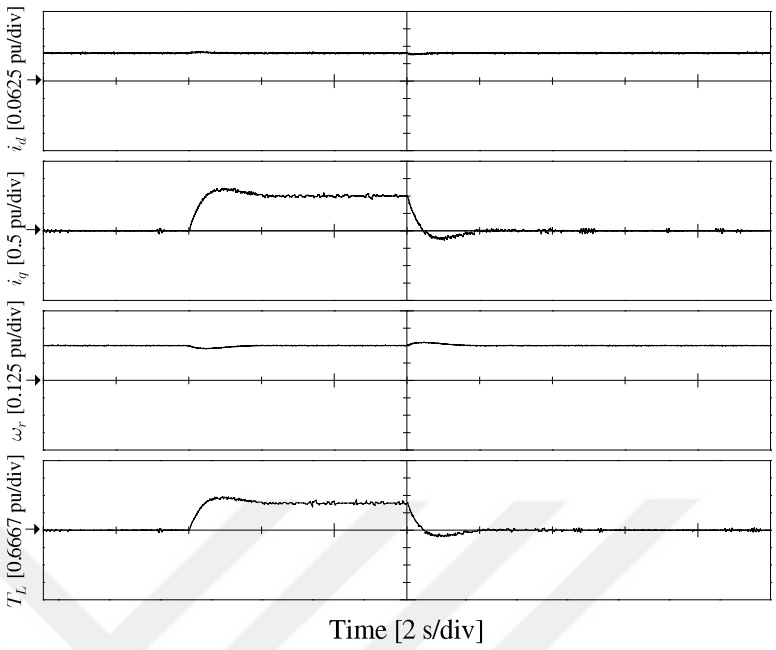

Figure VI.11. IFOC of IM performance under full load at 12.5 Hz (375 r/min) with 4 pulse encoder using OLS speed estimation.

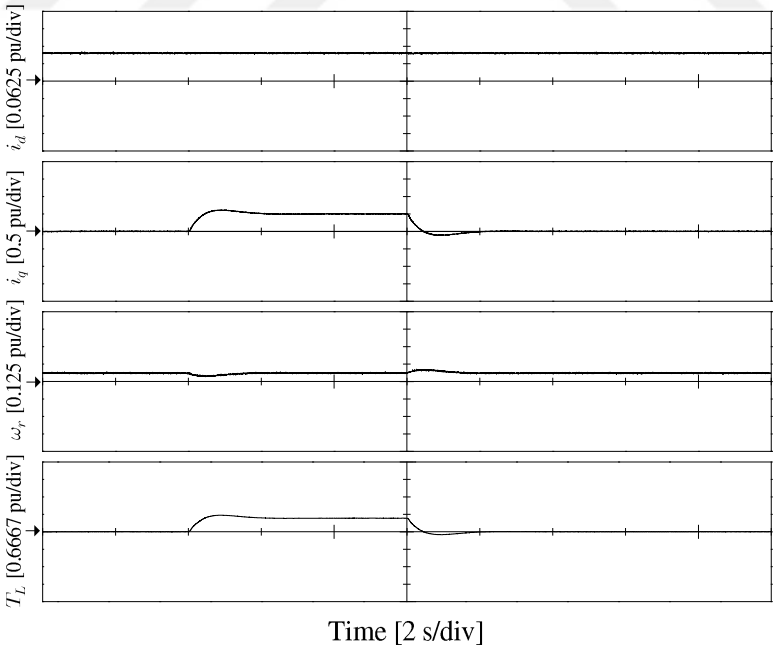

Figure VI.12. IFOC of IM performance under half load at 1.25 Hz (37.5 r/min) with 16 pulse encoder using OLS speed estimation.

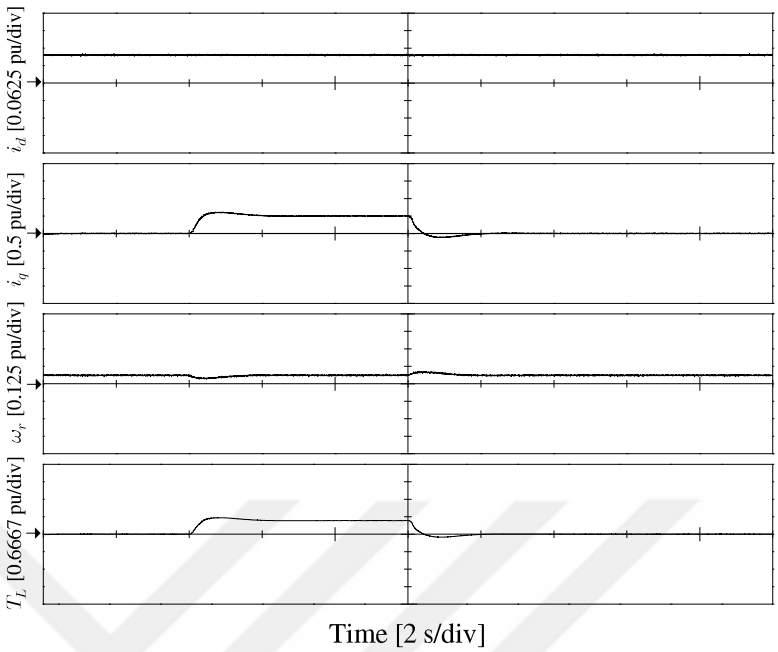

Figure VI.13. IFOC of IM performance under half load at 1.25 Hz (37.5 r/min) with 8 pulse encoder using OLS speed estimation.

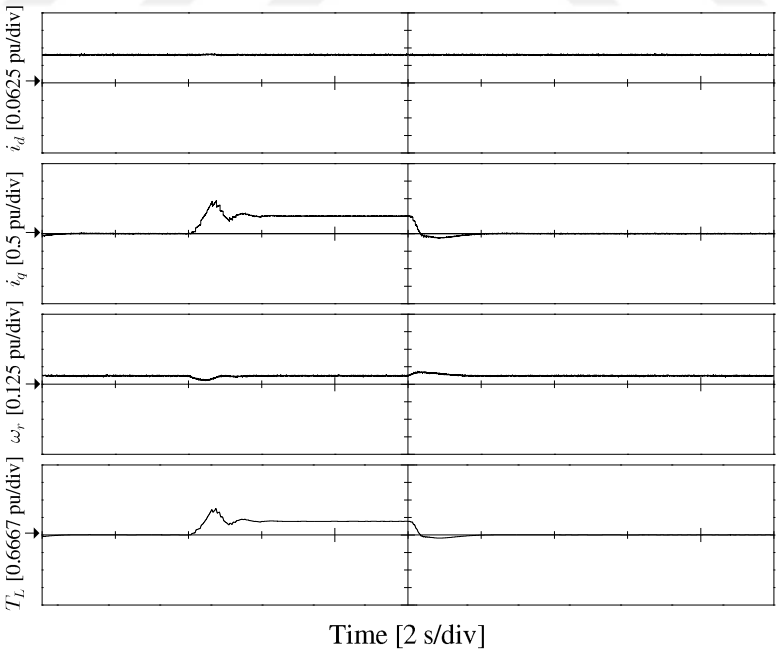

Figure VI.14. IFOC of IM performance under half load at 1.25 Hz (37.5 r/min) with 4 pulse encoder using OLS speed estimation.

Near-zero speed tests results under light-load are provided in Figure VI.15, Figure VI.16, and Figure VI.17 using OLS speed estimation. It is reported that 1–5 r/min range is achieved successfully with 16 and 32 pulse encoders with OLS. Steady-state phase current and speed wave-form of IFOC obtained from the DAC output at 5 r/min with 16 and 8 pulse encoders and at 10 r/min using 4 pulse encoder are given in Figure VI.15, Figure VI.16, and Figure VI.17, respectively. Speed wave-forms are pretty smooth and stable and phase currents are quite sinusoidal even for 4 pulse encoder case using OLS speed estimation method at very low speed range under light load (10% of full load).

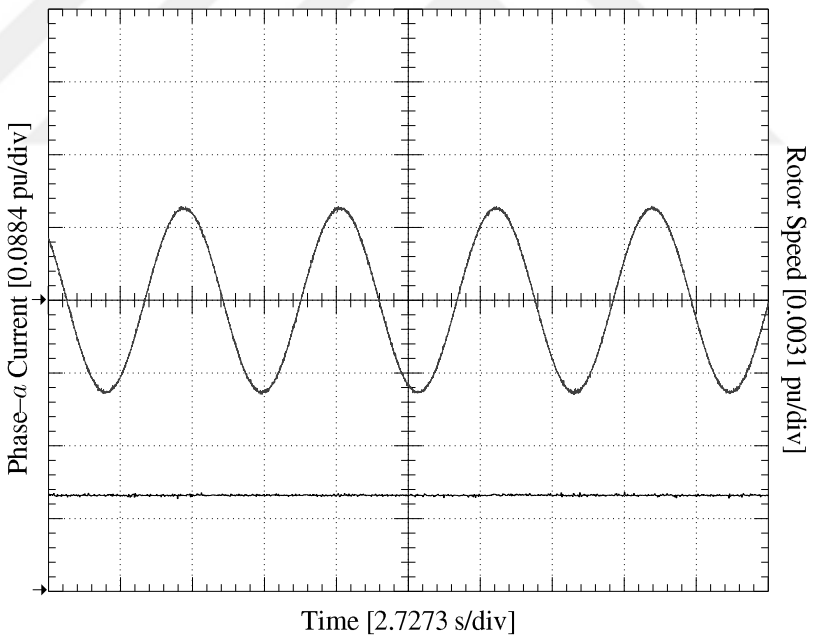

Figure VI.15. IFOC of IM performance at very low speed under light load (%10 of full load) with 16 (5 r/min) encoder using OLS speed estimation.

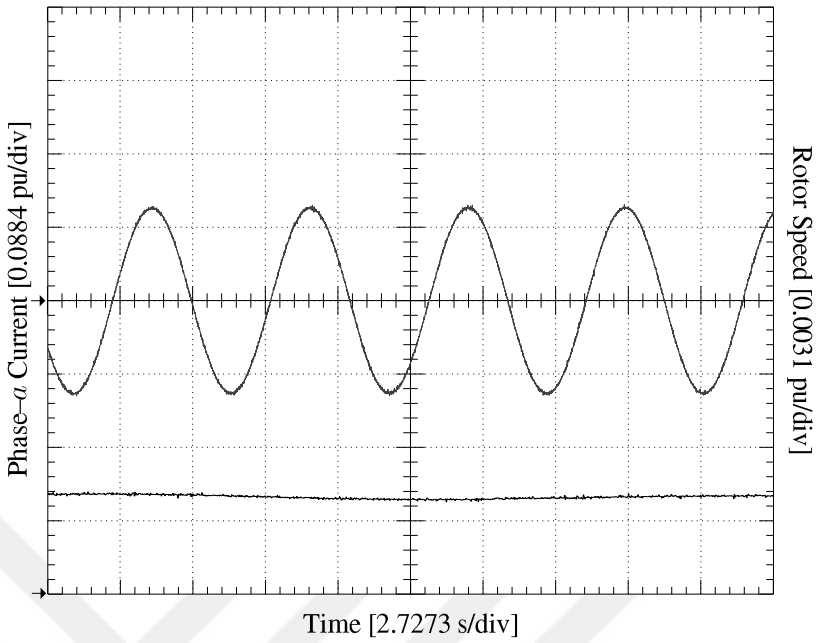

Figure VI.16. IFOC of IM performance at very low speed under light load (%10 of full load) with 8 (5 r/min) encoder using OLS speed estimation.

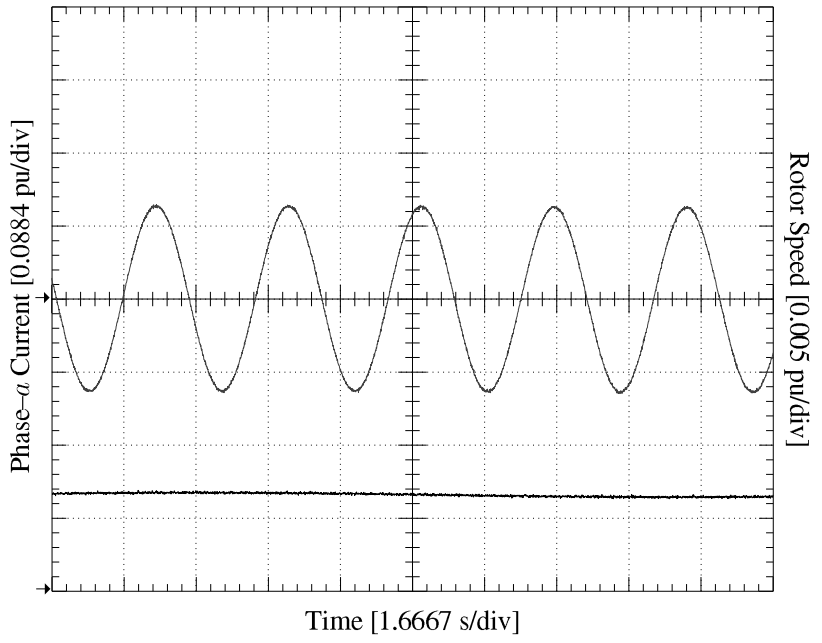

Figure VI.17. IFOC of IM performance at very low speed under light load (%10 of full load) with 4 (5 r/min) encoder using OLS speed estimation.

VII. SUMMARY AND CONCLUSIONS

This thesis has presented investigation, analysis and implementation of TMS320F28335 based IFOC of IM drive using low-resolution speed sensor at low and very low speed ranges by using both simple speed measurement and OLS speed estimation techniques. The minimum possible speed that IFOC algorithm runs without instability using OLS method with low-count encoders are figured out experimentally. It is also shown that IFOC algorithm with simple speed measurement and OLS speed estimation can be run with the resolution that a four pulse encoder module provides safely down to one digit rotor speed in rpm. Experimental tests regarding OLS speed estimation including start-up, four-quadrant, near zero speed, and under full, half, light and no load conditions with low-count encoders down to four pulse show that OLS speed estimation is capable of providing very good speed response especially at near zero speed region compared to simple speed measurement method.

REFERENCES

[1] G. Rizzoni, *Principles and Applications of Electrical Engineering*. 2008.

[2] A. Hughes., *Electric Motors and Drives Fundamentals, Types and Applications*, Fourth. Elsevier Ltd., 2013.

[3] S. B. Ozturk, "Modeling, Simulation and Analysis of low-cost direct torque control of PMSM using Hall-effect Sensors," Texas A&M University, 2005.

[4] V. Valkenburgh, *Basic Electricity*, Rev. ed. Indianapolis, Ind. : Prompt Publications, c1992., 1992.

[5] A. M. Trzynadlowski, *Control of Induction Motors*. Nevada, 2001.

[6] L. Ben-Brahim, S. Tadakuma, and a. Akdag, "Speed control of induction motor without rotational transducers," *IEEE Trans. Ind. Appl.*, vol. 35, no. 4, pp. 844–850, 1999.

[7] F.-Z. Peng and T. Fukao, "Robust speed identification for speed sensorless vector control of\ninduction motors," *Conf. Rec. 1993 IEEE Ind. Appl. Conf. Twenty-Eighth IAS Annu. Meet.*, 1993.

[8] B. Akin, U. Orguner, A. Ersak, and M. Ehsani, "A comparative study on non-linear state estimators applied to sensorless AC drives: MRAS and Kalman filter," *IECON Proc. (Industrial Electron. Conf.*, vol. 3, pp. 2148–2153, 2004.

[9] H. Ahn and D. Lee, "A New Bumpless Rotor-Flux Position Estimation Scheme for Vector-Controlled Washing Machine," *IEEE*, vol. 12, no. 2, pp. 466–473, 2016.

[10] S. Morimoto, M. Sanada, and Y. Takeda, "High-performance current-sensorless drive for PMSM and SynRM with only low-resolution position sensor," *IEEE*

Trans. Ind. Appl., vol. 39, no. 3, pp. 792–801, 2003.

[11] B. Akin, S. B. Ozturk, P. Niazi, H. A. Toliyat, and A. Goodarzi, “Low speed performance operation of induction motors drives using low-resolution speed sensor,” *IEEE Int. Symp. Ind. Electron.*, vol. 3, pp. 2110–2115, 2006.

[12] A. Slocum, *Precision Machine Design*. 1992.

[13] T. K. K. Mekid, Samir, *Introduction to Precision Machine Design and Error Assessment*. US, 2009.

[14] R. M. Kennel, “Encoders for simultaneous sensing of position and speed in electrical drives with digital control,” *IEEE Trans. Ind. Appl.*, vol. 43, no. 6, pp. 1572–1575, 2007.

[15] D. S. Nyce, *Linear Position Sensors: Theory and Application*. 2004.

[16] D. Byrd, “Closed-loop motor control : An introduction to rotary resolvers and encoders,” pp. 5–8, 2014.

[17] Honeywell, “Hall Effect Sensing and Application,” *Sens. Control*, pp. 1–5, 2011.

[18] Texas Instruments, “C2000 Digital Motor Controls,” no. October. pp. 1–221, 2012.

[19] B. Akin and M. Bhardwaj, “Sensored Field Oriented Control of 3-Phase Induction Motors,” 2013.

[20] E. R. Filho, “Three-phase Induction Motor Dynamic Mathematical Model,” in *IEEE*, 1997, vol. 2, no. 11, pp. 1–3.

[21] A. W. Leedy, “Simulink/Matlab dynamic induction motor model for use in undergraduate electric machines and power electronics courses,” in *Conference Proceedings - IEEE SOUTHEASTCON*, 2013, pp. 1–6.

[22] A. M. Trzynadlowski, *The Field Orientation Principle in Control of Induction*

Motors, vol. 27. Kluwer Academic Publishers, 1994.

[23] S. B. Ozturk, B. Akin, B. Harbor, and H. A. L. L. F. S. Ensors, "Low-Cost Direct Torque Control of Permanent Magnet Synchronous Motor Using Hall-Effect Sensors," in *IEEE*, 2006, pp. 667–673.

[24] M. F. Benkhoris, "Discrete speed estimation from a position encoder for motor drives," *6th Int. Conf. Power Electron. Var. Speed Drives*, vol. 1, no. 429, pp. 283–287, 1996.

[25] R. Petrella, M. Tursini, L. Peretti, and M. Zigliotto, "Speed measurement algorithms for low-resolution incremental encoder equipped drives: A comparative analysis," *Int. Aegean Conf. Electr. Mach. Power Electron. Electromotion ACEMP'07 Electromotion'07 Jt. Conf.*, pp. 780–787, 2007.

[26] C. A. Negrea, I. I. Incze, M. Imecs, A. V. Pop, and C. Szabo, "An improved speed identification method using incremental encoder in electric drives," *2012 IEEE Int. Conf. Autom. Qual. Testing, Robot. AQTR 2012 - Proc.*, pp. 536–540, 2012.

[27] A. C. Negrea, M. Imecs, I. L. Incze, A. Pop, and C. Szabo, "Error compensation methods in speed identification using incremental encoder," *EPE 2012 - Proc. 2012 Int. Conf. Expo. Electr. Power Eng.*, no. Epe, pp. 441–445, 2012.

[28] H. Abdi, "Least Squares," *Encycl. Res. Des.*, pp. 1–7, 2010.

APPENDIX A

Altivar 71 (Schneider Electric) settings for finding induction motor parameters for the proposed project

- **Main menu**

1. Drive Menu

Table A.1. Altivar 71 Schneider Electric settings for finding induction motor parameters.

1.1. Simply start	• 2/3 wire control	2 wire
	• Macro configuration	Stop/start
	• Standard motor frequency	50 Hz IEC
	• Rated Motor Power	From nameplate
	• Rated Motor Current	From nameplate
	• Rated Motor Voltage	From nameplate
	• Rated Motor Frequency	From nameplate
	• Rated Motor Speed in rpm	From nameplate
	• Max Frequency	60 Hz
	• Acceleration	3.0 sec
	• Deceleration	3.0 sec
	• Low speed	0 Hz
	• High speed	50 Hz
1.2. Monitoring	• HMI Frequency Reference	User defined

	• HMI Torque Reference	User defined
1.4. Motor control	Note: We can put motor nameplate ratings in here as well.	
	• Auto tuning	By this we can measure motor parameters i.e. R_s, i_{dr}, L_{fr}, T_{2r}, S, P.
	• Motor control type	SVC I
	• Vector control 2pt	No
	• IR compensation	100%
	• Slip compensation	100%
	• Output Phase rotation	ABC
	• Rpm increment	× 1 rpm
	• Noise reduction	Yes

1.6. Command	• Ref.1 channel	HMI
	• RV inhabitation	No
	• Stop key priority	Yes
	• Ref.2 switching	Channel 1 active
1.7. Application Functions	1.7.1 RAMP 1.7.2 Stop configuration 1.7.3 Torque control 1.7.4 Torque Limitations	

1.7.1. RAMP	• Ramp type	Linear
	• Ramp increment	0.1
	• Acceleration	3.0 sec
	• Deceleration	3.0 sec
	• Ramp 2 threshold	0.0 Hz
	• Ramp switch ass.	No
	• Dec. ramp adapt	Yes
1.7.2 Stop configuration	• Type of stop	Ramp stop
	• DOTD	Rmp
1.7.2. Torque control	• Trq/spd switching	Yes
	• Torque Ref. channel	HMI
	• Torque Ref. sign	No
	• Torque ratio	100%
	• Torque Ramp time	3.00 sec
	• Torque control stop	Speed
	• Positive dead band	10 Hz
	• Negative dead band	10 Hz
	• Torque control timeout	60.0 sec
	• Torque control fault mgt.	Alarm

Table A.2. Parameters and specifications of the IM.

Nominal torque (hp)	1
Number of poles	4
Rated voltage (V)	400
Rated speed (r/min)	1430
Rated frequency (Hz)	50
Stator resistance (Ω)	0.435
Rotor resistance (Ω)	0.815
Magnetizing impedance (Ω)	26.15
Leakage impedance (Ω)	0.75

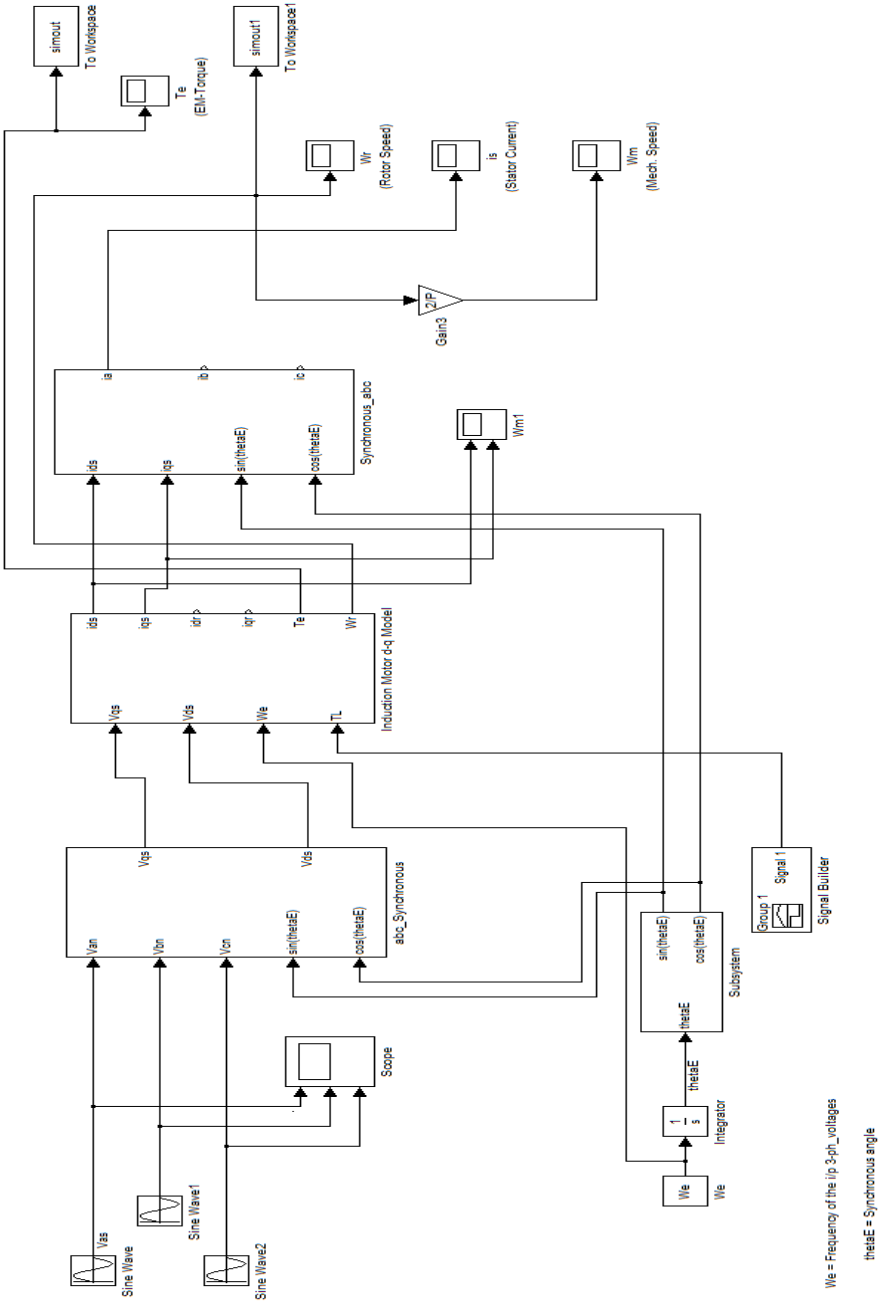

Figure A.1. Dynamic model of induction motor in MATLAB/Simulink model.

VITA

Saeed Ur Rehman received his Bachelor of Science degree from Cecos University of IT & Emerging Sciences, Peshawar Pakistan, in April 2012. He worked in Power Electronics and Energy Conversion (PEEC) Laboratory, in the Department of Electrical and Electronics Engineering at Okan University, Istanbul, Turkey, with Asst. Prof. Dr. Salih Barış Öztürk as his advisor. He is currently pursuing a M.Sc. degree in the same university.

He can be reached in care of:

Asst. Prof. Dr. Salih Barış Öztürk

Power Electronics and Energy Conversion (PEEC) Laboratory

Department of Electrical and Electronic Engineering

Okan University

Tuzla Campus, Istanbul 0 (216) 677 16 30 #2461